

INTERCUSP GEODESICS AND CUSP SHAPES OF FULLY AUGMENTED LINKS

ROCHY FLINT

ABSTRACT. We study the geometry of fully augmented link complements in S^3 by looking at their link diagrams. We extend the method introduced by Thistlethwaite and Tsvietkova [16] to fully augmented links and define a system of algebraic equations in terms of parameters coming from edges and crossings of the link diagrams. Combining it with the work of Purcell [15], we show that the solutions to these algebraic equations are related to the cusp shapes of fully augmented link complements. As an application we use the cusp shapes to study the commensurability classes of fully augmented links.

1. INTRODUCTION

Understanding the relationship between the combinatorics of a link diagram and the geometry and topology of its complement is an important problem and an active area of research. In this paper we study this relationship for an infinite family of links called *fully augmented links*. These are links obtained from a given link diagram by augmenting every twist region with a circle component and removing all twists, see Figure 1.

Thurston studied the interactions between geometry and combinatorics using ideal triangulations and gluing equations for hyperbolic link complements and 3-manifolds. The solutions to the gluing equations allow us to construct the discrete faithful representation of the fundamental group of the link complement to $\text{Isom}^+(\mathbb{H}^3)$ and help us to compute many geometric invariants. Although an ideal triangulation can be obtained from a link diagram easily, it is much harder to find solutions to the gluing equations. In addition, it is difficult to relate the geometric invariants obtained from the solutions of gluing equations to the diagrammatic invariants obtained from the link diagram.

In [16] Thistlethwaite and Tsvietkova used link diagrams to study the geometry of hyperbolic alternating link complements by implementing a method to construct a system of algebraic equations directly from the link diagram. The solutions to these equations allow them to construct the discrete faithful representation of the link group into $\text{Isom}^+(\mathbb{H}^3)$. We refer to their method as the T-T method. The idea of the T-T method is as follows: by looking at the faces of the link diagram, and assigning parameters to crossings and edges in every face, they find relations on the parameters using the geometry of the link complement, which determine algebraic equations, and the solutions to these equations have geometric information.

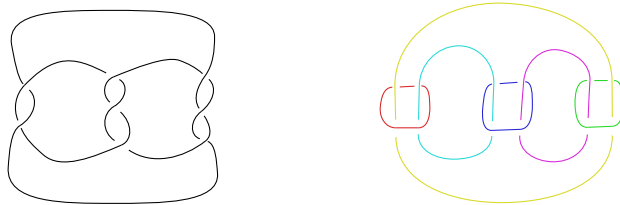


FIGURE 1. link K (left) and the corresponding fully augmented link L (right).

Throughout this paper we abbreviate fully augmented links to FALs. In this paper we show the following for FALs:

- (1) A way to extend the T-T method to FALs. This is the first application of the T-T method to an infinite class of non-alternating links. This is done in Proposition 3.1, Theorem 3.2, Lemma 3.3, and Lemma 3.4;
- (2) A new method to determine the cusp shapes of FAL complements using the solutions of the system of equations obtained from the T-T method. This is proved in Theorem 4.1 and Theorem 4.3;
- (3) A way to study commensurability of different classes of FALs. This is done in Theorems 5.6, 5.7, and 5.13;
- (4) A way to choose the geometric solutions i.e. the solution which enables us to construct the discrete, faithful representation, from the solutions of the system of equations obtained from the T-T method. We demonstrate this in Theorem 5.17.

This paper is divided into 5 sections. In §2 we give necessary background about FALs, the geometry of their complements, and introduce the T-T method for alternating links. We also give an example illustrating the T-T method on alternating links. In §3 we show that the T-T method can be extended to FALs, and illustrate with examples. In §4 we state our main theorem relating the cusp shapes to the intercuspidal geodesics, and give explicit examples. §5 discusses applications of our main theorems by studying the invariant trace fields, commensurability and finding geometric solutions to systems of equations in the T-T method for FALs.

1.1. Acknowledgements. This paper consists of results from my PhD dissertation. Many thanks to Abhijit Champanerkar for his invaluable support, innumerable conversations, and unlimited patience. I wish to thank Ilya Kofman and Walter Neumann for their constant support and advice. I also thank Jessica Purcell and Anastasiia Tsvietkova for helpful conversations, encouragement and their work which motivated this research project.

2. BACKGROUND

A *hyperbolic 3-manifold* M is a 3-manifold equipped with a complete Riemannian metric of constant sectional curvature -1 , i.e. the universal cover of M is \mathbb{H}^3 with covering translations acting as isometries. Equivalently, $M = \mathbb{H}^3/\Gamma$ where Γ is a torsion

free Kleinian group i.e. a discrete torsion-free subgroup of $\mathrm{PSL}(2, \mathbb{C}) = \mathrm{Isom}^+(\mathbb{H}^3)$. In this paper we assume that our hyperbolic 3-manifolds are complete, orientable and have finite hyperbolic volume. Hyperbolic 3-manifolds have a thick-thin decomposition that allows us to understand the topology of non-compact hyperbolic 3-manifolds. This decomposition consists of a thin part with tubular neighborhoods of closed geodesics and ends which are homeomorphic to a thickened torus.

A *cusps* of a hyperbolic 3-manifold is the thin end isometric to $T^2 \times [0, \infty)$ with the induced metric given as $ds^2 = e^{-2t}(dx^2 + dy^2) + dt^2$.

If $M = \mathbb{H}^3/\Gamma$, then M is non-compact if and only if Γ contains parabolic isometries (i.e. they have one fixed point on the sphere at infinity of \mathbb{H}^3), which correspond to the cusps of M . Distinct cusps of M correspond to distinct conjugacy classes of maximal parabolic subgroups of Γ . Note that the cross sectional tori $T^2 \times \{t\}$ are scaled Euclidean tori.

We say a link $K \in S^3$ is *hyperbolic* if its complement $S^3 - K$ is a hyperbolic 3-manifold. In a link complement, the cusps are the tubular neighborhoods of the component of the link with the link components deleted. The cusps lift to a set of horoballs with disjoint interiors in the universal cover \mathbb{H}^3 . For each cusp, the set of horoballs are identified by the covering transformations. Thurston's famous example of the figure-eight knot complement decomposing into two ideal tetrahedra [17] is the first example of finding the hyperbolic structure from a link diagram. Jeff Weeks implemented the computer program SnapPea which finds the geometric structure on link complements from link diagrams [18]. This was extended by Marc Culler and Nathan Dunfield to the program SnapPy [6].

Hyperbolic structures are useful to study knots and links using geometric invariants. One such invariant we will study in this paper is the *cusps shape*.

Definition 2.1. [11] A horospherical section of a cusp of a hyperbolic 3-manifold M is a flat torus. This torus is isometric to \mathbb{C}/Λ , for some lattice $\Lambda \subset \mathbb{C}$, and the ratio of two generators of Λ is the conformal parameter of the flat torus, which we call the *cusps shape* of the cusp of M . Choosing generators $[m]$ and $[\ell]$ of $\pi_1(T^2)$, the Euclidean structure on the torus is obtained by mapping $[m]$ and $[\ell]$ to Euclidean translations $T_1(z) = z + \mu$ and $T_2(z) = z + \lambda$ respectively, where μ and $\lambda \in \mathbb{C}$. Then μ and λ generate the lattice Λ and the cusps shape is obtained as λ/μ .

The cusps shape gives us very important information about links. Given a specific link diagram, we can compute the cusps shape by drawing the link diagram in SnapPy [6], which computes the hyperbolic structure on its complement and many geometric invariants including the cusps shape. For example, SnapPy gives a numerical value of the cusps shapes of the Hamantash Link (See Figure 10) as $1.5 + 1.32287565553i$. Below we will develop another way to compute the cusps shape for FALs directly from the diagram of the links using what we call the T-T polynomial.

Definition 2.2. Two hyperbolic 3-manifolds are *commensurable* if they have a common finite-sheeted cover.

The cusps shape gives us key information that will enable us to analyze whether certain links are commensurable. The cusps shapes are algebraic numbers and generate

a number field called the *cuspid field*. Although the cusp shape depends on the choice of generators of the peripheral subgroup, a different choice changes it by an integral Möbius transformation, hence the cusp field is independent of choices of generators. The cusp field is a commensurability invariant [10]. Hence cusp shapes can be used to determine commensurability of two links complements.

2.1. Fully Augmented Links. The class of links that we will be studying is called fully augmented links.

Definition 2.3. A link diagram is *prime* if for any simple closed curve in the plane that intersects a component transversely in two points the simple closed curve bounds a subdiagram containing no crossings. See Figure 2(a).

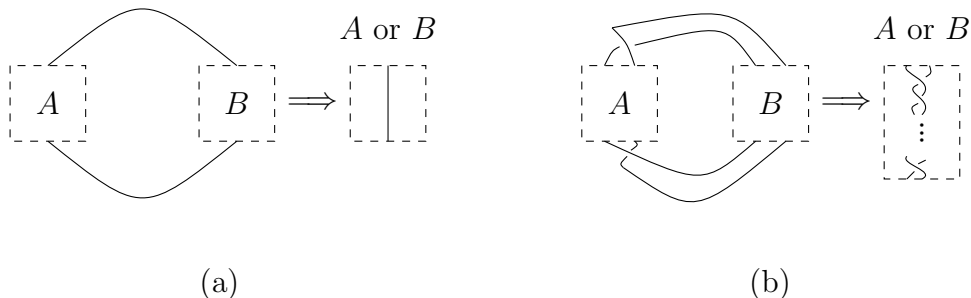


FIGURE 2. (a) Prime diagram (b) Twist Reduced diagram

Definition 2.4. In a link diagram, a string of bigons, or a single crossing is called a *twist region*. A link diagram is *twist reduced* if for any simple closed curve in the plane that intersects the link transversely in four points, with two points adjacent to one crossing and the other two points adjacent to another crossing, the simple closed curve bounds a subdiagram consisting of a (possibly empty) collection of bigons strung end to end between these crossings. See Figure 2(b).

Definition 2.5. A *fully augmented link* (FAL) is a link that is obtained from a diagram of a link K as follows:

- (1) augment every twist region with a circle component (called a *crossing circle*),
- (2) get rid of all full twists, and
- (3) remove all remaining half-twists. See Figure 3. A diagram obtained above will be referred to as a FAL diagram. The diagram obtained after step (2) is called a FAL diagram with half-twists.

Thus the FAL diagram consists of link components in the projection plane and crossing circle components that are orthogonal to the projection plane and bound twice punctured discs. In [15] Purcell studied the geometry of FALs using a decomposition of the FAL complement into a pair of totally geodesic hyperbolic right-angled ideal polyhedra. We will describe how the geodesic faces of these polyhedra can be seen on the FAL diagrams.

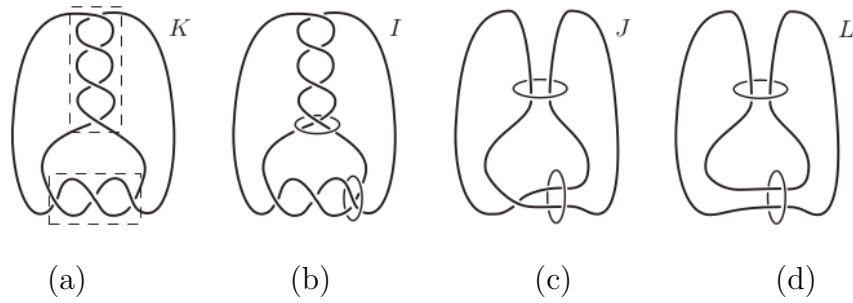


FIGURE 3. (a) Link diagram K (b) Crossing circles added at each twist region (c) Augmented Link with all full twists removed (d) fully augmented link L [13].

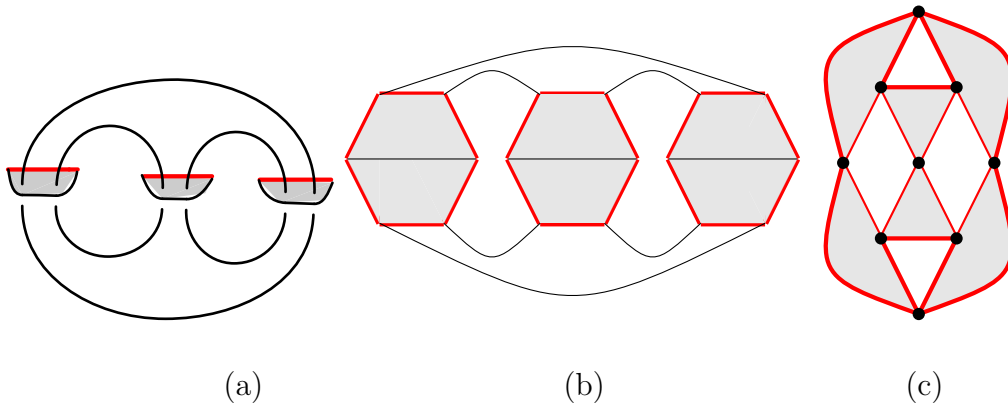


FIGURE 4. Polyhedral decomposition of a FAL using the cut-slice-flatten method. (a) Cut the FAL complement in half along the projection plane. This also cuts the crossing circles and the bounded twice punctured discs in half. (b) Slice open the half discs and flattened down on the projection plane. (c) Polyhedron P_L is obtained by contracting the link components to ideal vertices.

FAL, while interesting in their own right, enable us to study the geometry of the original knot or link it's built from.

Theorem 2.6. [15, 2, 5] *A fully augmented link is hyperbolic if and only if the associated knot or link diagram is non-splittable, prime, twist reduced, with at least two twist regions.*

We will only consider hyperbolic FALs in this paper.

2.1.1. *The Cut-Slice-Flatten Method and Polyhedron P_L .* Given a FAL diagram L , we can obtain the polyhedra decomposition by using a construction given by Agol and D. Thurston in [9] called the *cut-slice-flatten method*. Assume that the twice punctured discs are perpendicular to the plane. First, cut the link complement in half along the projection plane, which cuts the twice punctured disc bounded by the crossing circle

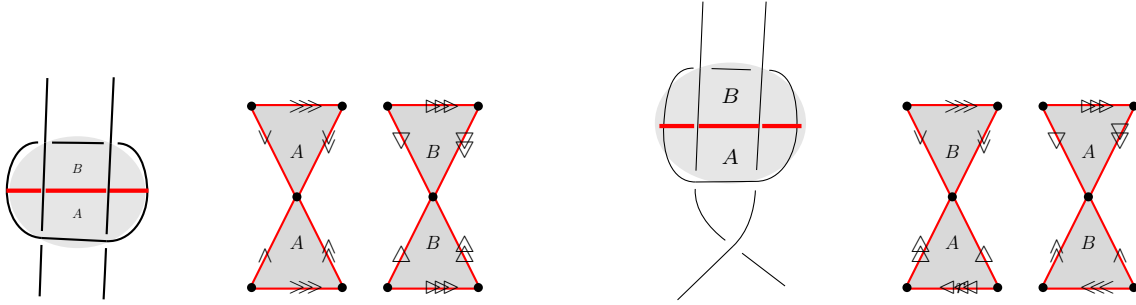


FIGURE 5. Gluing bowties without half-twist (leftmost three figures) and when half-twist are present (rightmost three figures).

into half. This creates a pair of polyhedra, see Figure 4(a). For each half, slice open the half disc like a pita bread and flatten it down on the projection plane, see Figure 4(b). Lastly, shrink the link components to ideal vertices, see Figure 4(c). This gives us two copies of a polyhedron which we denote as P_L . For each crossing circle we get a *bowtie* on each copy of P_L , which consists of two triangular faces that share the ideal vertex corresponding to the crossing circle component. The cut-slice-flatten method is part of the proof of Proposition 2.2 in [15], which we state below:

Proposition 2.7. [15, 5] *Let L be a hyperbolic FAL diagram. There is a decomposition of $S^3 \setminus L$ into two copies of geodesic, ideal, hyperbolic polyhedron P_L with the following properties.*

- (1) *Faces of P_L can be checkerboard colored, with shaded faces corresponding to bowties, and white faces corresponding to the regions of the FAL components in the projection plane.*
- (2) *Ideal vertices of P_L are all 4-valent.*
- (3) *The dihedral angle at each edge of P_L is $\frac{\pi}{2}$.*

2.1.2. *Gluing the Polyhedra.* For FAL with or without half-twists the polyhedron P_L is the same. The difference is in how they glue up. For FAL without half-twist the shaded faces glue up such that the bowties on each polyhedron glue to each other, see Figure 5 leftmost, and then the white faces on each polyhedron get glued to their respective copies. Whereas in the case a half-twist occurs, the shaded faces get glued to the opposite shaded face on the other polyhedron, see Figure 5 rightmost, and then the white faces on each polyhedron get glued to their respective copies. Right handed and left handed twists produce the same link complement due to the presence of the crossing circle as one can add/delete full twists without changing the link complement. In §4 we use this gluing to study the fundamental domain of a cusp.

2.1.3. *Circle Packings and Cusp Shapes.*

Definition 2.8. A *circle packing* is a finite collection of circles inside a given boundary such that no two overlap and some (or all) of them are mutually tangent.

The geometry of FAL complements is studied using the hyperbolic structure on P_L . Since all faces of P_L are geodesic, for each face, the hyperbolic plane it lies on determines a circle or line in $\mathbb{C} \cup \{\infty\}$. Purcell showed that there is a corresponding circle packing for the white geodesic faces of P_L , and a dual circle packing for the geodesic shaded faces of P_L . We can visualize P_L if you place the two circle packings on top of one another, and intersect it with half-spaces in \mathbb{H}^3 .

In [15] Purcell described a technique to compute cusp shapes of FALs by examining the circle packings and the gluing of polyhedra. The main result of this paper is that we can extend the T-T method to fully augmented links, and determine the cusp shapes of FALs by solving an algebraic system of equations, see §4. Since the equations are obtained directly from the FAL diagram, we can directly relate the combinatorics of FAL diagrams and the geometry of FAL complements.

2.2. T-T Method. We will work in the upper half-space model of hyperbolic 3-space \mathbb{H}^3 .

Definition 2.9. [16] A diagram of a hyperbolic link is *taut* if each associated checkerboard surface is incompressible and boundary incompressible in the link complement, and moreover does not contain any simple closed curve representing an accidental parabolic.

The taut condition implies that the faces in the diagram correspond to ideal polygons in \mathbb{H}^3 with distinct vertices. Let L be a taut, oriented link diagram of a hyperbolic link. A *crossing* arc is an arc which runs from the overcrossing to the undercrossing. Let R be a face in L with n crossings. Then R corresponds to an ideal polygon F_R in \mathbb{H}^3 as follows:

- (1) Distinct edges of L around the boundary of R lift to distinct ideal vertices in \mathbb{H}^3 because of the no accidental parabolic condition in Definition 2.9.
- (2) The lifts of the crossing arcs can be straightened out in \mathbb{H}^3 to geodesic edges giving the ideal polygon F_R . See Figure 6.

Remark 2.10. Although the vertices of F_R are ideal and the edges are geodesic, the face of F_R need not be geodesic, i.e F_R needs not lie on a hyperbolic plane in \mathbb{H}^3 .

There are two types of parameters we will focus on in R . The first type of parameter is assigned to each crossing in R and is known as the *crossing label*, also referred to in the literature as *crossing geodesic parameter*, or *intercusp geodesic parameter*, denoted by ω_i . The second parameter we will focus on is assigned to the edges of L in R , and is known as an *edge label*, also referred to in the literature as *translational geodesic parameter*, or *edge parameter* and denoted by u_j . See Figure 6.

Remark 2.11. When we are in the diagram we refer to ω_i and u_j as crossing and edge labels respectively. When we are in \mathbb{H}^3 we refer to them as intercusp and translational parameters, respectively.

We will choose a set of horospheres in \mathbb{H}^3 such that for every cusp the meridian curve on the cross-sectional torus has length one. Furthermore, we will choose one horosphere to be the Euclidean plane $z = 1$. It follows from results of Adams on waist

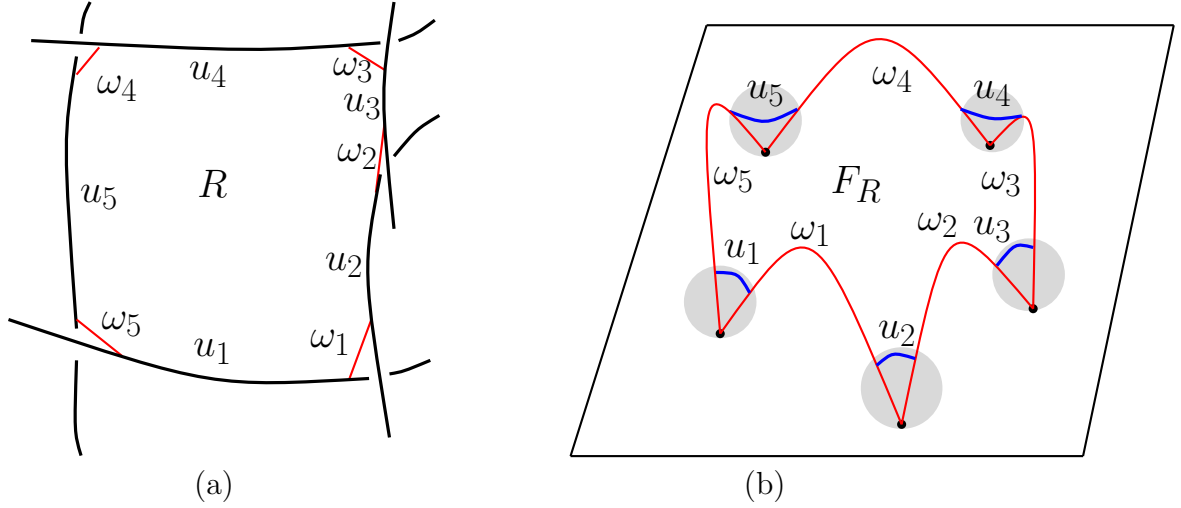


FIGURE 6. (a) Face (region) R in a link diagram. (b) The corresponding ideal polygon F_R in \mathbb{H}^3 .

size of hyperbolic 3-manifolds [3] that the horoballs are at most tangent and have disjoint interiors.

The lift of the crossing arc is a geodesic γ in \mathbb{H}^3 which is an edge of the ideal polygon F_R and which travels from the center of one horoball to the center of an adjacent horoball. For each horosphere the meridional direction along with geodesic γ defines a hyperbolic half-plane. The intercusp parameter ω_γ , is defined as $|\omega_\gamma| = e^{-d}$ where d is the hyperbolic distance between the horoballs along the geodesic γ , and the argument of ω_γ is the dihedral angle between these two half-planes, both of which contain γ . ω_γ encodes information about the intercusp translation taking into account distance and angles formed by parallel transport. The isometry that maps one horoball to another is represented up to conjugation by the 2×2 matrix $\begin{bmatrix} 0 & \omega_\gamma \\ 1 & 0 \end{bmatrix}$ in $GL(2, \mathbb{C})$, which maps horosphere H_2 to horosphere H_1 in Figure 7(a).

For each edge inside a region R we assign *edge labels*. The edges lift to ideal vertices of the polygon F_R in \mathbb{H}^3 . The edge label u_j represent the translation parameter along the horosphere centered at that ideal vertex that travels from one intercusp geodesic to another. From u_j we can find the distance traveled along a horoball, and the direction of travel. Since the edge label is a translation, up to conjugation it is represented by a 2×2 matrix: $\begin{bmatrix} 1 & \epsilon_j u_j \\ 0 & 1 \end{bmatrix}$, where ϵ_j is positive if the direction of the edge in the diagram is the same as the direction of travel along the region, and negative otherwise, see Figure 6(b), the matrix is an isometry translating one endpoint of the u_i curve to the other end along the horosphere, i.e. it maps p_i to q_i or q_i to p_i along horosphere H_i , see Figure 7(b).

We use the following conventions.

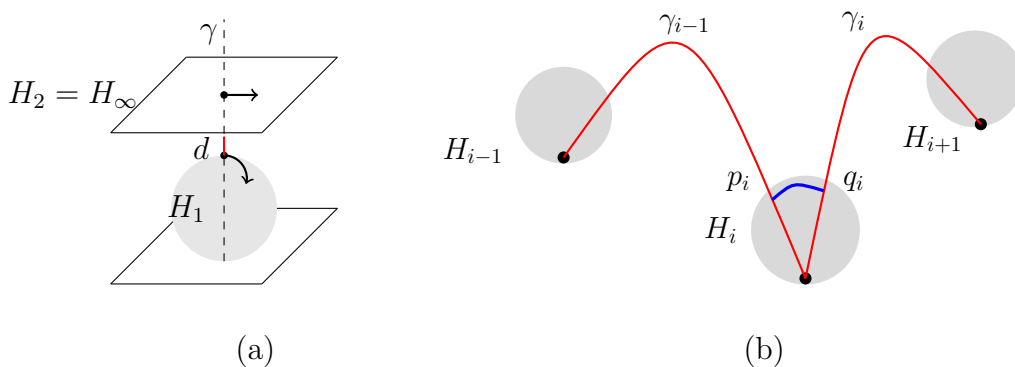


FIGURE 7. (a) The isometry for the intercusp geodesic maps H_∞ to H_1 . (b) The isometry that maps along the translational geodesic points p_i to q_i or the reverse.

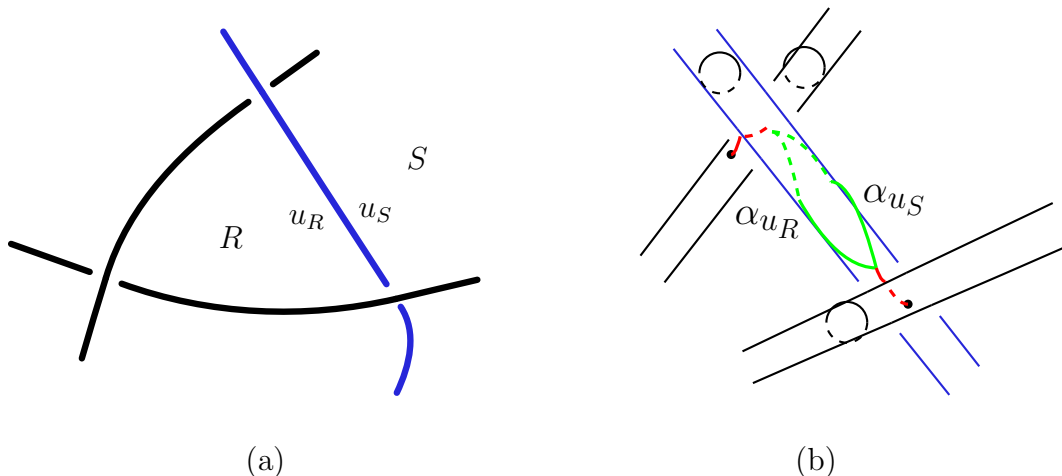


FIGURE 8. (a) The relation between the two sides of an edge. (b) The corresponding meridian loop along the solid torus boundary giving the relation.

- (1) The basis of peripheral subgroups is the canonical meridian and longitude. The meridian is oriented using the right hand screw rule with respect to the orientation of the link.
- (2) The length of meridians along the horospherical cross section on a cusp are 1 [3]. Consequently, there is a natural relationship between the two faces incident to the diagram that share an edge in the diagram: let R and S be adjacent regions that share an edge u , then the edge labels u_R and u_S satisfy $u_R - u_S = \pm 1$ or 0 depending on whether the edge is going from overpass to underpass, underpass to overpass, or staying leveled respectively from within region R . See Figure 8.
- (3) The edge labels inside a bigon are zero.

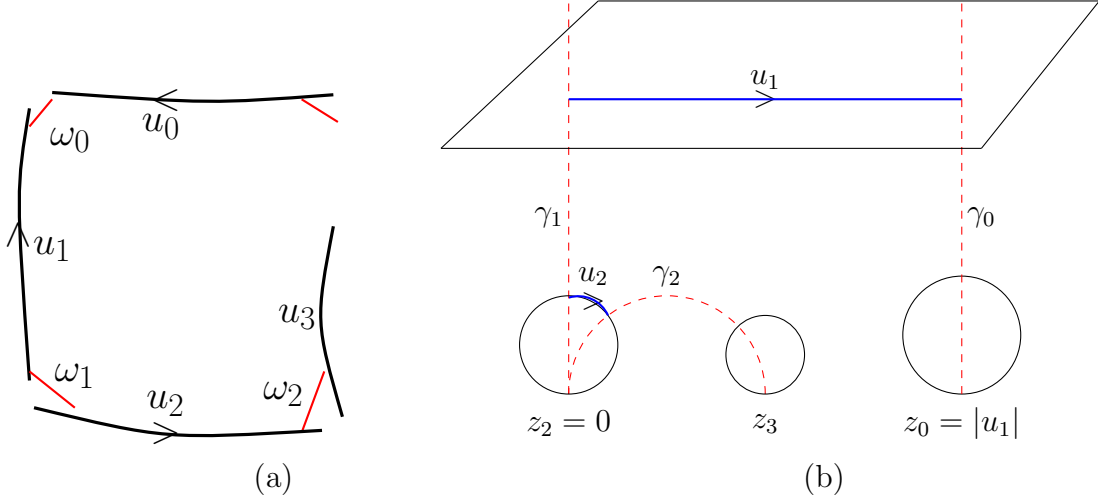


FIGURE 9. (a) Edge and crossing labels in the link diagram. (b) The corresponding translational and intercusp geodesics in \mathbb{H}^3 .

Remark 2.12. For convention 2 above, this relationship holds if the actual region in the diagram corresponds to the ideal polygonal face in \mathbb{H}^3 as described above. In this case, the translation on either side of the region will start and end with the same intercusp geodesics as the other side. However, below we will see that for fully augmented links, the faces coming from the crossing circles will not be the faces from the diagram directly, but will require the polyhedral decomposition of the complement first. In this case the edges will not share the same intercusp geodesics, thus the above relationship will not necessarily hold, and will require modification.

Definition 2.13. Let the ideal vertices of the n -sided ideal polygon F_R corresponding to the face R be z_1, \dots, z_n . We will assign a shape parameter to each edge of the polygon as follows: Let γ_i be a geodesic edge between ideal vertices z_i and z_{i+1} then its *shape parameter* ξ_i is defined as

$$\xi_i = \frac{(z_{i-1} - z_i)(z_{i+1} - z_{i+2})}{(z_{i-1} - z_{i+1})(z_i - z_{i+2})},$$

which is the cross-ratio of four consecutive vertices of F_R .

Thistlethwaite and Tsvietkova show that the above shape parameter can be written in terms of crossing and edge labels in Proposition 4.1 in [16]. For our purposes all the faces in our class of links will have total geodesic faces as we shall see below.

Proposition 2.14. [16] *Up to complex conjugation, $\xi_i = \frac{\pm\omega_i}{u_i u_{i+1}}$ where the sign is positive if both edges are directed away or both are directed toward the crossing, negative if one edge is directed into the crossing and one is directed out.*

Proof. Let z_0, z_1, z_2, z_3 be four consecutive ideal vertices in \mathbb{H}^3 that correspond to the edges with edge labels u_0, u_1, u_2, u_3 respectively in the link diagram L , See Figure 9. We can always perform an isometry and let z_0 be placed at $|u_1|$, z_1 at ∞ where

the horoball H_∞ is at Euclidean height 1, z_2 at $(0, 0, 0)$. Let γ_0 connect z_0 to z_1 , correspond to ω_0 in L , γ_1 be the geodesic connecting z_1 to z_2 correspond to ω_1 in L and γ_2 connect z_2 to z_3 correspond to ω_2 in L . The horoball H_2 has diameter $|\omega_1|$ since the hyperbolic distance between H_∞ and H_2 is $\log \frac{1}{|\omega_1|}$ and $|\omega| = e^{-d}$. In [16] T-T showed that $u_2 = \frac{|\omega_1|}{|z_3|}$. Thus the shape parameter ξ_1 is

$$\xi_1 = \frac{(z_0 - z_1)(z_2 - z_3)}{(z_0 - z_2)(z_1 - z_3)} = \frac{z_3}{z_0} = \frac{\frac{|\omega_1|}{u_2}}{u_1} = \frac{|\omega_1|}{u_1 u_2}.$$

If either u_1 or u_2 exclusively were going in the opposite direction then it will cause the shape parameter to be of different sign. \square

Let R_i be a face in L , which corresponds to F_{R_i} in the ideal polygon. Fix F_{R_i} , we can perform an isometry sending ideal vertices z_{i-1} , z_i , and z_{i+1} to 1, ∞ , and 0 respectively, then z_{i+2} will be placed at ξ_i . Since the region closes up, the collection of shape parameters for each region determines the isometry class of the associated ideal polygon. The shape parameters ξ_i satisfy algebraic equations amongst themselves. For example, for a 3-sided region the shape parameters are equal to each other and are equal to 1, while in a 4-sided region the sum of consecutive shape parameters is equal to 1. For regions with $n \geq 5$ we use Proposition 4.2 in [16] to determine the algebraic equations in terms of crossing and edge labels.

For each region in the diagram there is an alternating sequence of edges and crossings until the region closes up. The product of the corresponding matrices is a scalar multiple of the identity. Consequently, we have a system of equations whose solution allows us to construct a discrete faithful representation of the complement. We state Proposition 4.2 in [16].

Proposition 2.15. *Let R be a region of an oriented link diagram with $n \geq 3$ sides, and, starting from some crossing of R , let*

$$u_1, \omega_1, u_2, \omega_2, \dots, u_n, \omega_n$$

be the alternating sequence of edge and crossing labels for R encountered as one travels around the boundary of the region. Also, for $1 \leq i \leq n$ let $\epsilon_i = 1$ (resp. $\epsilon_i = -1$) if the direction of the edge corresponding to u_i is with (resp. against) the direction of travel. Then the equation for R is written as

$$\prod_{i=1}^n \left(\begin{bmatrix} 0 & \omega_i \\ 1 & 0 \end{bmatrix} \begin{bmatrix} 1 & \epsilon_i u_i \\ 0 & 1 \end{bmatrix} \right) \sim \begin{bmatrix} 1 & 0 \\ 0 & 1 \end{bmatrix}.$$

This can be done for each region of L , thus we have algebraic equations for each face R of L in terms of crossing and edge labels, the solutions to the algebraic equations allow us to construct the discrete faithful representation of the link group into $PSL_2(\mathbb{C})$.

It is proved in [16] that the solutions to the above system of equations is discrete. Thus we can eliminate the variables and reduce this system of equations to a 1-variable polynomial, referred to as the *T-T polynomial*. Neumann-Tsvietkova [12] related the solutions to the invariant trace field of the link complement.

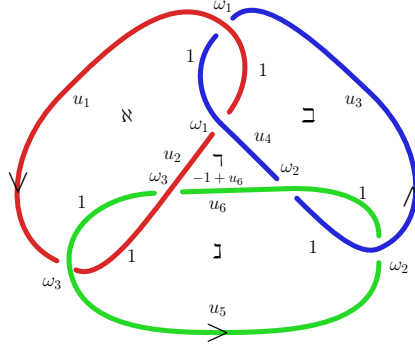


FIGURE 10. Hamantash Link

2.3. Example: Hamantash Link. Region \aleph : This is a four-sided region with shape parameters:

$$\xi_1 = \frac{\omega_1}{u_1}, \quad \xi_2 = \frac{\omega_1}{u_2}, \quad \xi_3 = \frac{\omega_3}{u_2}, \quad \xi_4 = \frac{\omega_3}{u_1}.$$

Thus the equations are:

$$\frac{\omega_1}{u_1} + \frac{\omega_1}{u_2} = 1, \quad \frac{\omega_1}{u_2} + \frac{\omega_3}{u_2} = 1, \quad \frac{\omega_3}{u_2} + \frac{\omega_3}{u_1} = 1, \quad \frac{\omega_3}{u_1} + \frac{\omega_1}{u_1} = 1$$

solving gives us the relations

$$u_1 = u_2 = 2\omega_1 = 2\omega_3, \quad \text{and} \quad \omega_1 = \omega_3.$$

Region \beth : This is a four-sided region with shape parameters:

$$\xi_1 = \frac{\omega_1}{u_4}, \quad \xi_2 = \frac{\omega_1}{u_3}, \quad \xi_3 = \frac{\omega_2}{u_3}, \quad \xi_4 = \frac{\omega_2}{u_4}.$$

Thus the equations are:

$$\frac{\omega_1}{u_4} + \frac{\omega_1}{u_3} = 1, \quad \frac{\omega_1}{u_3} + \frac{\omega_2}{u_3} = 1, \quad \frac{\omega_2}{u_3} + \frac{\omega_2}{u_4} = 1, \quad \frac{\omega_2}{u_4} + \frac{\omega_1}{u_4} = 1$$

solving gives us the relations

$$u_3 = u_4 = 2\omega_1 = 2\omega_2, \quad \text{and} \quad \omega_1 = \omega_2.$$

Region \beth : This is a four-sided region with shape parameters:

$$\xi_1 = \frac{\omega_3}{u_6}, \quad \xi_2 = \frac{\omega_2}{u_6}, \quad \xi_3 = \frac{\omega_2}{u_5}, \quad \xi_4 = \frac{\omega_3}{u_5}.$$

Thus the equations are:

$$\frac{\omega_3}{u_6} + \frac{\omega_2}{u_6} = 1, \quad \frac{\omega_2}{u_6} + \frac{\omega_2}{u_5} = 1, \quad \frac{\omega_2}{u_5} + \frac{\omega_3}{u_5} = 1, \quad \frac{\omega_3}{u_5} + \frac{\omega_3}{u_6} = 1$$

solving gives us the relations

$$u_5 = u_6 = 2\omega_2 = 2\omega_3, \quad \text{and} \quad \omega_2 = \omega_3.$$

Region ∇ : This is a three-sided region with edge labels $-1 + u_2$, $-1 + u_4$, $-1 + u_6$.

$$\xi_1 = \frac{-\omega_1}{(-1 + u_2)(-1 + u_4)} = 1, \quad \xi_2 = \frac{-\omega_2}{(-1 + u_4)(-1 + u_6)} = 1, \quad \xi_3 = \frac{-\omega_3}{(-1 + u_6)(-1 + u_2)} = 1$$

solving these equations we get the T-T polynomial as

$$4\omega_1^2 - 3\omega_1 + 1 = 0$$

thus

$$\omega_i = \frac{3}{8} \pm \frac{\sqrt{7}}{8}i, \quad u_i = \frac{3}{4} \pm \frac{\sqrt{7}}{4}i.$$

Neumann-Tsvietkova proved in [12] that one of the roots of the polynomial should give us the invariant trace field.

We can check the linear dependence using mathematica or pari-gp. It is suggested in [16] that the geometric solution will be the one that produces the highest volume, but finding the volume from the solutions can be difficult. In §5 we will show how to find the geometric solution for the class of fully augmented links.

Using Snap the invariant trace field for the Hamantash link is

$$x^2 - x + 2, \quad x = \frac{1}{2} + \frac{\sqrt{7}}{2}i \quad \text{and} \quad \omega_1 = \frac{1+x}{4}.$$

3. T-T METHOD AND FAL

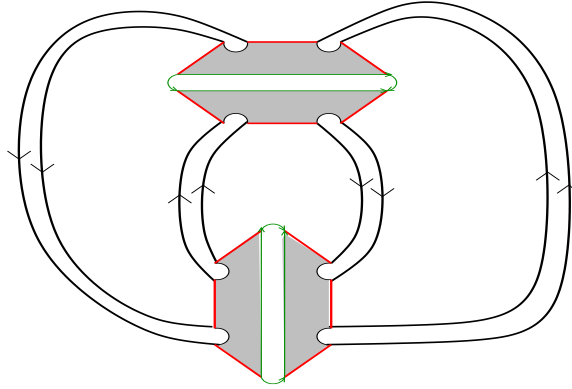
In this section we show that the T-T method can be effectively extended to the class of fully augmented links. Our extension of the T-T method will be on a trivalent graph which is the intermediate step between the FAL diagram and the polyhedron P_L . We denote the *planar trivalent graph* T_L , for example see Figure 4(b). T_L is in fact the ideal polyhedron P_L , truncated at the ideal vertices, along with the orientations on the links of the vertices. Since the vertices are all 4-valent, the link of the vertices are all rectangles which tessellate the cusp torus. Thinking of the long thin rectangular pieces as thick edges in Figure 11 (T_L for Borromean FAL), one gets the trivalent graph T_L . The components of the link diagram and the crossing geodesics are both visible on T_L . The crossing geodesics are on the boundary of the hexagonal regions corresponding to the bowties. We will assign the edge labels and the crossing labels on this type of diagram for the T-T method to work.

In order to use the T-T method we need to ensure that it can be applied to the class of FALs. The tautness condition on the diagram is to ensure that the faces in the link diagram correspond to ideal polygons in \mathbb{H}^3 with distinct vertices.

Proposition 3.1. *Let L be a FAL diagram, then the planar trivalent graph T_L is taut.*

Proof. Let L be a hyperbolic FAL. By Lemma 2.1 in [15], the following surfaces are embedded totally geodesic surfaces in the link complement:

- (1) twice punctured discs coming from the regions bounded by the crossing circles and punctured by two strands in the projection plane, and
- (2) the surfaces in the projection plane.

FIGURE 11. T_L for Borromean FAL

Embedded totally geodesic surfaces are Fuchsian and Thurston's trichotomy for surfaces in 3-manifolds implies a surface can either be quasifuchsian, accidental, or semi-fibered [7]. This implies they do not contain any accidental parabolics. We have a checkerboard coloring by shading the discs coming from the regions bounded by the crossing circles, and leaving the surfaces in the projection plane white. Thus by definition, the checkerboard surfaces of T_L are incompressible and boundary incompressible. Hence T_L is taut. \square

Since the regions of T_L correspond to geodesic faces in \mathbb{H}^3 , the definitions for crossing and edge labels in the T-T method, the corresponding matrices, the shape parameters and equations of Propositions 2.14 and 2.15 hold for T_L . The fundamental difference is in the relationship between parameters for edges incident to adjacent faces as will be discussed below.

3.1. Thrice Punctured Sphere. The twice punctured disc bounded by the crossing circle is geodesic and has the hyperbolic structure of the thrice punctured sphere formed by gluing two ideal triangles. So we will refer to the twice punctured discs as thrice punctured spheres from now on. Let L be a FAL, then L contains at least two crossing circles. This implies $S^3 \setminus L$ contains at least two thrice punctured spheres. We will first study how the T-T method defines parameters on the thrice punctured sphere and use this as a basic building block for FALs.

The thrice punctured sphere has three components, two strands that lie in the projection plane, and another circle component known as a crossing circle that encircles the two other strands. The thrice punctured sphere is known to be totally geodesic constructed by gluing two ideal triangles together along their edges [1]. There are two cases based on the orientation: one where the strands in the projection plane are parallel and the other when they are anti-parallel. On T_L the thrice punctured sphere corresponds to a hexagon, and on P_L it corresponds to a bowtie. We will study the part of T_L corresponding to the hexagon.

Theorem 3.2. (1) *The crossing labels on opposite sides of the augmented circles with parallel strands in the link diagram will be equal and the intercusp geodesic along the projection plane equals $-1/4$.*

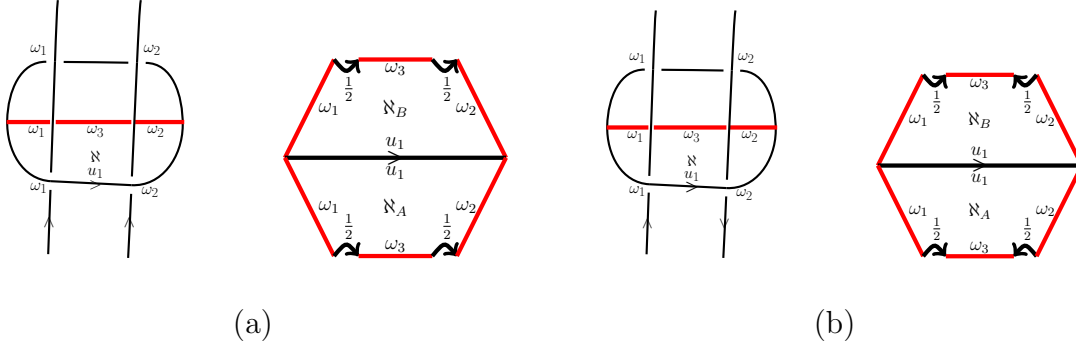


FIGURE 12. (a) Thrice punctured sphere with parallel strands with the intercusp geodesics penciled in and corresponding region in T_L . (b) Thrice punctured sphere with anti-parallel strands with the intercusp geodesics penciled in and corresponding region in T_L . Here we can see the intercusp and translational parameters in the T_L regions.

- (2) *The crossing labels on opposite sides of the augmented circles with anti-parallel strands in the link diagram will differ by sign and the intercusp geodesic along the projection plane equals $1/4$.*

Proof. For each crossing circle there are four crossing labels ω_i . The two labels that share a bigon are equivalent since the region collapses and has the same geodesic arc going from horoball to horoball [16]. For the relationship between the two crossing labels that don't share a bigon we have two cases:

Case 1: Parallel strands in the link diagram

As the cusp torus for the crossing circle is cut in half, the translation parameters coming from the longitudinal strands in the projection plane will also be cut in half and are $1/2$ keeping with the convention that the meridional curve along the cross sectional torus has length 1 and keeping with the right hand screw rule. For region \mathfrak{N}_A in Figure 12(a) right, we have shape parameters:

$$\xi_1 = \frac{\omega_1}{\frac{1}{2}u_1} = 1, \quad \xi_2 = \frac{-\omega_3}{\frac{1}{2} \times \frac{1}{2}} = 1, \quad \xi_3 = \frac{\omega_2}{\frac{1}{2}u_1} = 1,$$

solving these equations gives us the relations

$$\omega_3 = -\frac{1}{4}, \quad \omega_1 = \omega_2, \quad \text{and} \quad u_1 = 2\omega_1.$$

Using Proposition 2.15 we can check that these parameters are correct. Starting from the edge ω_1 in the left side of region \mathfrak{N}_A and traveling counterclockwise we have:

$$\begin{bmatrix} 0 & \omega_1 \\ 1 & 0 \end{bmatrix} \begin{bmatrix} 1 & 1/2 \\ 0 & 1 \end{bmatrix} \begin{bmatrix} 0 & -1/4 \\ 1 & 0 \end{bmatrix} \begin{bmatrix} 1 & \frac{1}{2} \\ 0 & 1 \end{bmatrix} \begin{bmatrix} 0 & \omega_2 \\ 1 & 0 \end{bmatrix} \begin{bmatrix} 1 & -u_1 \\ 0 & 1 \end{bmatrix} = \begin{bmatrix} -\frac{\omega_1}{2} & 0 \\ 0 & -\frac{\omega_1}{2} \end{bmatrix}.$$

Case 2: Anti-parallel strands in the link diagram.

Notice here that the translation parameters coming from the longitudinal strands will be $\frac{1}{2}$ but their directions differ each going according to the right hand screw rule

and the orientation on the strands, see Figure 12(b). For Region \aleph_A we have shape parameters

$$\xi_1 = \frac{\omega_1}{\frac{1}{2}u_1} = 1, \quad \xi_2 = \frac{-\omega_2}{\frac{1}{2}u_1} = 1, \quad \xi_3 = \frac{\omega_3}{\frac{1}{2} \times \frac{1}{2}} = 1$$

solving these equations gives us the relations

$$\omega_3 = \frac{1}{4}, \quad \omega_1 = -\omega_2, \quad \text{and} \quad u_1 = 2\omega_1.$$

Using Proposition 2.15, starting from the red edge ω_1 in the left side of region \aleph_A and traveling counterclockwise we have:

$$\begin{bmatrix} 0 & \omega_1 \\ 1 & 0 \end{bmatrix} \begin{bmatrix} 1 & 1/2 \\ 0 & 1 \end{bmatrix} \begin{bmatrix} 0 & 1/4 \\ 1 & 0 \end{bmatrix} \begin{bmatrix} 1 & -\frac{1}{2} \\ 0 & 1 \end{bmatrix} \begin{bmatrix} 0 & \omega_2 \\ 1 & 0 \end{bmatrix} \begin{bmatrix} 1 & -u_1 \\ 0 & 1 \end{bmatrix}$$

substituting in the above relations = $\begin{bmatrix} -\frac{\omega_1}{2} & 0 \\ 0 & -\frac{\omega_1}{2} \end{bmatrix}$. □

3.2. Adaptation of T-T Method for FAL Diagram. All the shaded faces on a FAL diagram come from thrice punctured spheres, and have parameters as determined in Theorem 3.2. Hence to set up the T-T equations, we only need to understand the edge and crossing parameters on the regions in the projection plane. These regions are the white faces which have boundary alternating between the crossing geodesics and strands of the link diagram, except when it intersects the crossing circle. At the intersection of the region and the crossing circle, the boundary goes across a meridian of the crossing circle, see Figure 11. Thus with an adjustment, we can write down the equations directly from the FAL diagram, without using T_L .

Lemma 3.3. *For each crossing circle, the two translational geodesics that correspond to the parts of the crossing circle component that bound the bigons, one going from ω_1 to ω_1 and the other going from ω_2 to ω_2 correspond to the meridional curve for that component, thus both are oriented the same way and are equal to 1.*

Proof. The part of the cusp torus corresponding to a crossing circle lies on the hexagon in T_L , such that the meridians lie flat in the projection plane. The orientations on the meridians are obtained by the right hand screw rule. The meridians on opposite sides of the crossing circle are homotopic and are oriented as in Figure 13(b). □

Consequently, starting from a FAL diagram, we can reorient parts of the crossing circle on the FAL diagram to agree with the orientations on the meridians. See Figure 13(c). With this adjustment we can now write the T-T equations directly from the FAL diagrams without using the trivalent graph T_L .

Now we need to analyze the relationship between edge labels coming from adjacent regions of an edge.

Lemma 3.4. *The edge labels on opposite sides of an edge coming from the longitudinal strands without a half-twist in the FAL diagram are equal.*

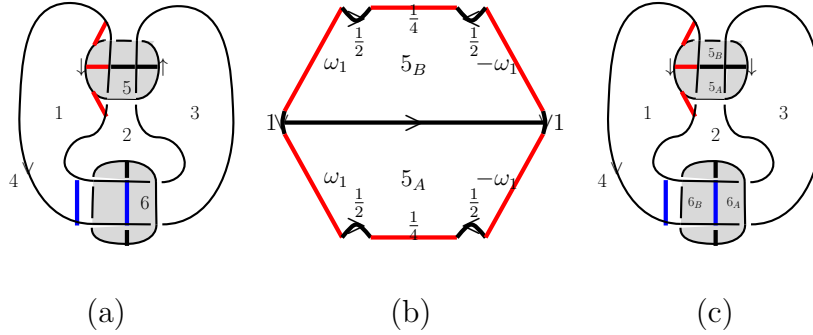


FIGURE 13. (a) FAL diagram with the orientations. (b) A portion of T_L after the cut-slice-flatten. (c) The manipulation on the diagram where the orientation for one side of the crossing circle is flipped.

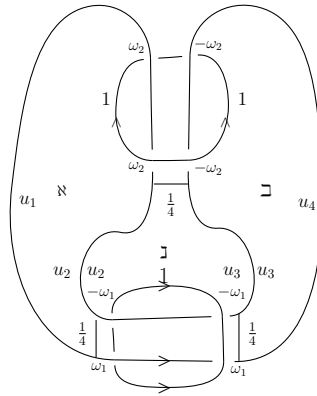


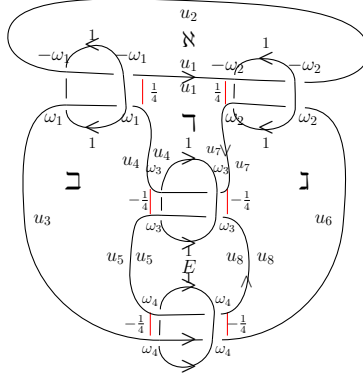
FIGURE 14. Borromean ring FAL with crossing and edge parameters.

Proof. Purcell showed how the cusps for FAL are tiled by rectangles [15]. Since the white faces on the two polyhedra are glued by identity, these rectangles can be seen in between the white faces on T_L , see Figure 11. The parts of the longitude corresponding to the adjacent regions are homotopic across the sliced torus. Hence they are equal. \square

In [15], Purcell showed that the complements of a FAL with and without a half-twist have the same polyhedral decomposition, but with different gluing on shaded faces. Thus the faces of the regions of a FAL diagram with half-twist do not represent white faces of P_L . So for FAL with half-twists we will take T_L the same as the one for the corresponding FAL without half-twists. We look at faces of T_L , we can find the intercusped geodesic parameters and translational parameters from analyzing the shear that is caused by the half-twist gluing. This will be done below when we look at the cusps in §4.

3.3. Examples.

3.3.1. *Borromean Ring FAL.* See Figure 14. Recall, for a 3-sided region all $\xi_i = 1$.

FIGURE 15. FAL_{4_1}

Region \aleph :

$$\xi_1 = \frac{-\omega_2}{u_1} = 1, \quad \xi_2 = \frac{-\omega_2}{u_2} = 1, \quad \xi_3 = \frac{-\frac{1}{4}}{u_1 u_2} = 1,$$

$$\implies u_1 = u_2 = -\omega_2 \quad \text{and} \quad u_1^2 = -\frac{1}{4} \quad \implies \quad u_1 = \pm \frac{i}{2}.$$

Region \beth :

$$\xi_1 = \frac{-\omega_2}{u_3} = 1, \quad \xi_2 = \frac{-\omega_2}{u_4} = 1, \quad \xi_3 = \frac{-\frac{1}{4}}{u_3 u_4} = 1,$$

\implies

$$u_3 = u_4 = -\omega_2 = \pm \frac{i}{2}.$$

Region \beth :

$$\xi_1 = \frac{-\omega_1}{u_3} = 1, \quad \xi_2 = \frac{-\omega_1}{u_2} = 1, \quad \xi_3 = \frac{-\frac{1}{4}}{u_2 u_3} = 1,$$

\implies

$$u_2 = u_3 = -\omega_1 = \pm \frac{i}{2}.$$

3.3.2. FAL_{4_1} . We denote the FAL shown in Figure 15 as FAL_{4_1} .

Region \aleph :

This is a four-sided region with shape parameters:

$$\xi_1 = \frac{-\omega_1}{u_2}, \quad \xi_2 = \frac{-\omega_2}{u_2}, \quad \xi_3 = \frac{-\omega_2}{u_1}, \quad \xi_4 = \frac{-\omega_1}{u_1}.$$

The sum of consecutive shape parameters are 1.

$$\frac{-\omega_1}{u_2} - \frac{\omega_2}{u_2} = 1, \quad \frac{-\omega_2}{u_2} - \frac{\omega_2}{u_1} = 1, \quad \frac{-\omega_2}{u_1} - \frac{\omega_1}{u_1} = 1, \quad \frac{-\omega_1}{u_1} - \frac{\omega_1}{u_2} = 1$$

solving gives us the relations

$$u_1 = u_2 = -2\omega_1 = -2\omega_2, \quad \text{and} \quad \omega_1 = \omega_2.$$

Region \beth :

This is a four-sided region with shape parameters:

$$\xi_1 = \frac{-\frac{1}{4}}{u_3 u_5}, \quad \xi_2 = \frac{-\omega_1}{u_3}, \quad \xi_3 = \frac{-\omega_1}{u_4}, \quad \xi_4 = \frac{-\frac{1}{4}}{u_4 u_5}.$$

Thus we have equations:

$$\frac{-\frac{1}{4}}{u_3 u_5} - \frac{\omega_1}{u_3} = 1, \quad \frac{-\omega_1}{u_3} - \frac{\omega_1}{u_4} = 1, \quad \frac{-\omega_1}{u_4} - \frac{\frac{1}{4}}{u_4 u_5} = 1, \quad \frac{-\frac{1}{4}}{u_4 u_5} - \frac{\frac{1}{4}}{u_3 u_5} = 1$$

solving gives us the relations $u_4 = u_3 = -2\omega_1$, and $u_5 = \frac{1}{4\omega_1}$

Region \mathbb{J} :

$$\xi_1 = \frac{-\frac{1}{4}}{u_8 u_6}, \quad \xi_2 = \frac{-\frac{1}{4}}{u_8 u_7}, \quad \xi_3 = \frac{-\omega_2}{u_7}, \quad \xi_4 = \frac{-\omega_2}{u_6}$$

This is a four-sided region with equations:

$$\frac{-\frac{1}{4}}{u_8 u_6} - \frac{\frac{1}{4}}{u_8 u_7} = 1, \quad \frac{-\frac{1}{4}}{u_8 u_7} - \frac{\omega_2}{u_7} = 1, \quad \frac{-\omega_2}{u_7} - \frac{\omega_2}{u_6} = 1, \quad \frac{-\omega_2}{u_6} - \frac{\frac{1}{4}}{u_8 u_6} = 1$$

solving gives us the relations

$$u_6 = u_7 = -2\omega_2, \quad \text{and} \quad u_8 = \frac{1}{4\omega_2}.$$

Region \mathbb{K} :

$$\xi_1 = \frac{-\frac{1}{4}}{u_4 u_1}, \quad \xi_2 = \frac{-\frac{1}{4}}{u_1 u_7}, \quad \xi_3 = \frac{\omega_3}{u_7}, \quad \xi_4 = \frac{\omega_3}{u_4}$$

This is a four-sided region with equations:

$$\frac{-\frac{1}{4}}{u_4 u_1} - \frac{\frac{1}{4}}{u_1 u_7} = 1, \quad \frac{-\frac{1}{4}}{u_1 u_7} + \frac{\omega_3}{u_7} = 1, \quad \frac{\omega_3}{u_7} + \frac{\omega_3}{u_4} = 1, \quad \frac{\omega_3}{u_4} - \frac{\frac{1}{4}}{u_4 u_1} = 1$$

solving gives us the relations

$$u_4 = u_7 = 2\omega_3, \quad \text{and} \quad u_1 = -\frac{1}{4\omega_3}.$$

Region E : This is a four-sided region with shape parameters:

$$\xi_1 = \frac{-\omega_4}{u_5}, \quad \xi_2 = \frac{\omega_3}{u_5}, \quad \xi_3 = \frac{\omega_3}{u_8}, \quad \xi_4 = \frac{-\omega_4}{u_8}.$$

Thus the equations are:

$$\frac{-\omega_4}{u_5} + \frac{\omega_3}{u_5} = 1, \quad \frac{\omega_3}{u_5} + \frac{\omega_3}{u_8} = 1, \quad \frac{\omega_3}{u_8} - \frac{\omega_4}{u_8} = 1, \quad \frac{-\omega_4}{u_8} - \frac{\omega_4}{u_5} = 1$$

solving gives us the relations

$$u_5 = u_8 = 2\omega_3 = -2\omega_4, \quad \text{and} \quad \omega_3 = -\omega_4.$$

Using the fact that opposite sides of an edge are equal, we get

$$\omega_1 = \pm \frac{\sqrt{2}}{4}i.$$

4. FAL CUSP SHAPES

In [15] Purcell described a method to compute the cusp shapes for each cusp of a FAL using the polyhedral decomposition, by lifting the ideal vertex corresponding to a crossing circle to ∞ , constructing a circle packing and computing the radii of each circle.

In Theorem 4.1 below we prove that the extension of the T-T method to FALs in §3 enable us to compute cusp shapes in a simpler way, by solving algebraic equations derived directly from the FAL diagram, without constructing the polyhedral decomposition, and circle packings.

Theorem 4.1. *Let L be a FAL diagram and let ω be the parameter of the crossing geodesic for a crossing circle C of L .*

- (1) *If L has no half-twist at C , then the cusp shape of C is 4ω .*
- (2) *If L has a RH half-twist at C , then the cusp shape of C is $\frac{4\omega}{1+2\omega}$.*
- (3) *If L has a LH half-twist at C , then the cusp shape of C is $\frac{4\omega}{1-2\omega}$.*

Remark 4.2. The FAL complements with RH half-twist and LH half-twist are isometric as a RH half-twist can be changed to a LH half-twist in presence of a crossing circle by adding a full twist, which is a homeomorphism. However the canonical longitude for the crossing circle is different in each case, thus we get a different cusp shape.

Proof. We will determine the longitude and meridian curves in the fundamental domain for the given crossing circle. Let L be a FAL and C be a crossing circle. Let $S^3 - L = P_1 \cup P_2$, where P_1 and P_2 are isometric to the right angled polyhedron P_L described in Proposition 2.7. The twice punctured disc bounded by C becomes a bowtie on P_L and the ideal point corresponding to C is the center of the bowtie. Let p denote the ideal point corresponding to C , since the faces of P_L are geodesic, they lie on hyperbolic planes, which are determined by circles or lines on $\mathbb{C} \cup \infty$. The four faces incident to p are two white faces and two shaded faces. Correspondingly we have two tangent circles in the white circle packing, and two tangent circles in the dual shaded circle packing, see Figure 16(b).

Superimposing the two circle packings, and taking the point p to ∞ , the four circles tangent to p become lines that form the rectangle of the cusp on each polyhedron P_1 and P_2 . Let H_∞ denote the horizontal plane corresponding to the horosphere centered at p . See Figure 16 (c). All other circles lie inside this rectangle, since the circles are at most tangent to one another and do not overlap. To find the cusp shape we need to study the fundamental domain of the cusp.

Case 1: Purcell showed that for FAL without a half-twist present, the fundamental domain for the cusp torus for C is formed by two rectangles attached along a white edge (representing a white face).

Let's describe the longitude and meridian curves along the crossing circle component of the FAL. Let s', r', t', q' denote the points on H_∞ that are directly above s, r, t, q respectively, translated along respective crossing geodesics ω_i . See Figure 16(b). The

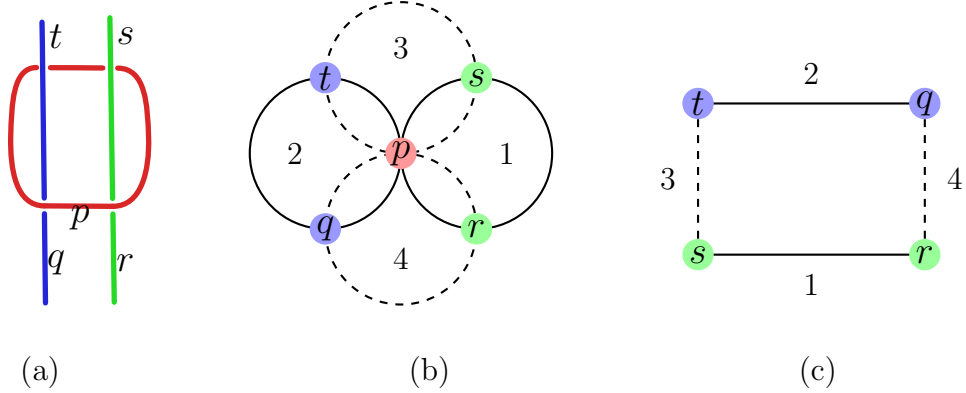


FIGURE 16. (a) Thrice punctured sphere without half-twist. (b) Solid circles representing the white faces and dashed circles representing the shaded faces at an ideal point arising from a crossing circle. (c) The rectangle formed by taking p to ∞ .

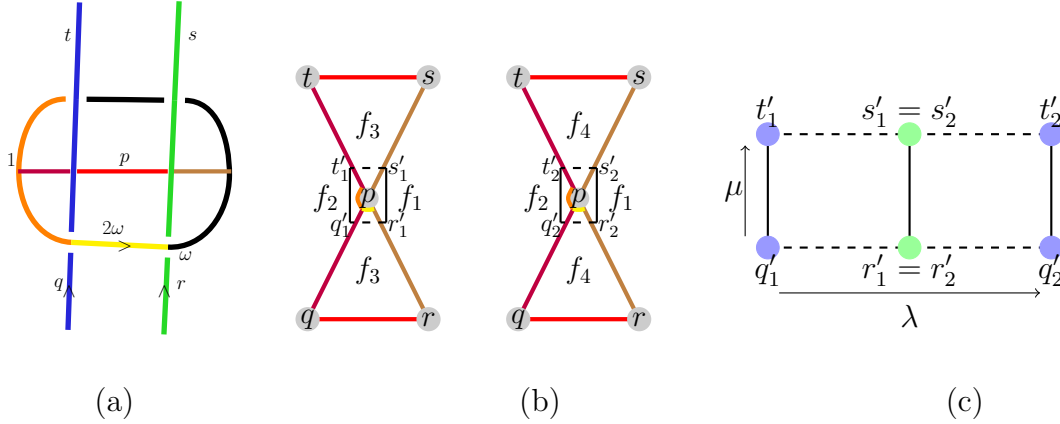


FIGURE 17. (a) Finding λ and μ for the cusp coming from the crossing circle on the diagram. (b) Cusp view on bowtie. (c) Fundamental domain for C .

fundamental domain is formed by taking two copies of the rectangle $s'r'q't'$ glued along the edge $s'r'$. The lift of the meridian is $s'r'$, and the longitude is double the curve $s't'$.

From the computations of the thrice punctured sphere in Section 3.1 edge parameter u_1 is isometric to geodesic $s't'$ which is the translation parameter along the horoball at hand and is 2ω . Since it is double in the actual cusp, the longitude parameter is 4ω . The translation parameter $s'r'$ is isometric to the meridian and is 1. Therefore, the cusp shape $\frac{\lambda}{\mu} = \frac{4\omega}{1}$, see Figure 17.

Case 2: for FAL with half-twists present, i.e. the crossing circle cusps that bound a half-twist will be tiled by rectangles but the fundamental domain will be a parallelogram due to a shear in the universal cover, its longitude curve will run along the shaded face (same as the case without a half-twist present) which is 4ω . The meridian

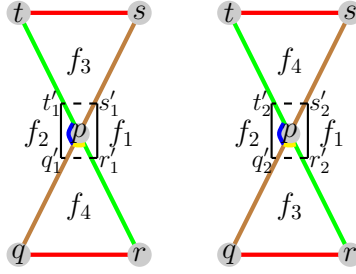


FIGURE 18. Gluing in Half-twist

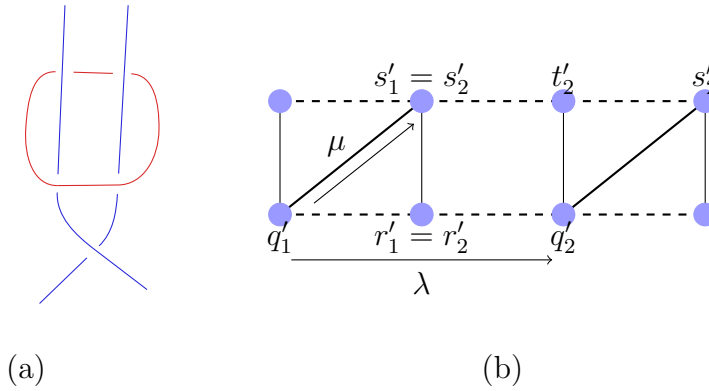


FIGURE 19. (a) TPS with RH half-twist. (b) The corresponding fundamental domain of the cusp due to the RH half-twist.

curve will run diagonally across since it takes one step along a white face and one step along a shaded face. This is due to a twist in the gluing of the shaded faces. s'_2 will be identified with q'_1 , and t'_2 will not be identified with q'_2 . There are two cases: The twist goes with a RH half-twist, see Figure 19(a), where the meridian goes diagonal increasing from left to right, thus it's $1 + 2\omega$ so the cusp shape is $\frac{4\omega}{1 + 2\omega}$. When the twist goes with the LH half-twist, see Figure 20(b), the diagonal is decreasing from left to right, it goes one step down which is -2ω and one step across which is 1, thus it's $1 - 2\omega$ and the cusp shape is $\frac{4\omega}{1 - 2\omega}$. \square

Note that the imaginary part of the cusp shape will always be positive.

The cusp shapes for the strands in the projection plane can also be determined from the labels in the diagram.

Theorem 4.3. *For a FAL without a half-twist, the cusp shape for a component in the projection plane will be the sum of the edge labels as one goes around the strand.*

Proof. In [13] Purcell showed that the component in the projection plane is tiled by a sequence of rectangles two for each segment of a component which is then glued along the shaded edge as one goes around the strand. See Figure 21. For each component in

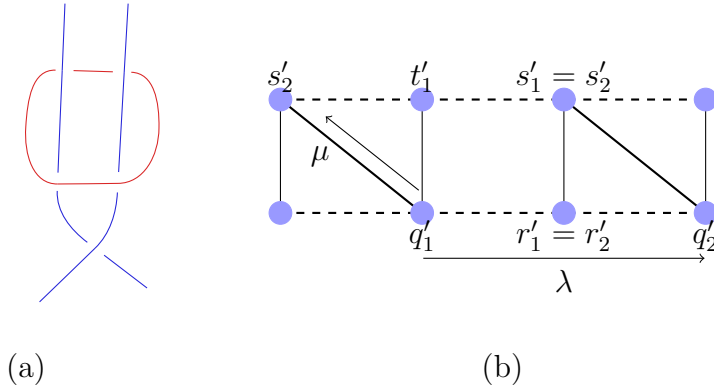


FIGURE 20. (a) TPS with LH half-twist. (b) The corresponding fundamental domain of the cusp due to the LH half-twist.

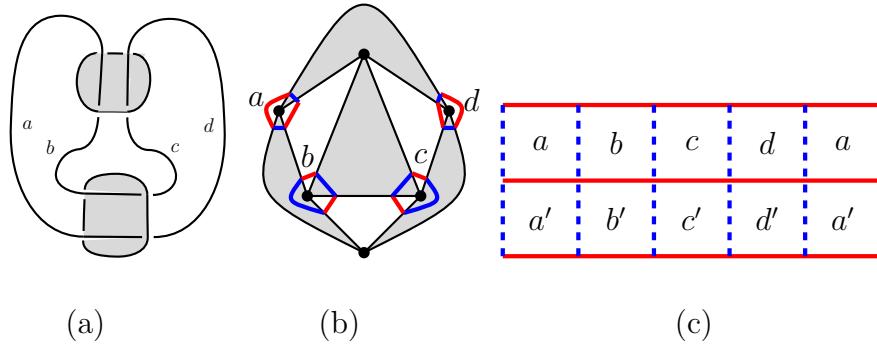


FIGURE 21. (a) $D(L)$ (b) Corresponding P_L with cusps from strands in projection plane drawn in. (c) The fundamental domain of corresponding cusp.

the projection plane there is a cusp that is tiled by rectangles coming from each portion along the component. Two identical rectangles are glued along a white edge for the upper and lower polyhedra. Then along the shaded edge the portion of the component adjacent will be glued along the shaded edge. The meridian is by convention 1, where we have a $\frac{1}{2}$ for the meridional segment along each shaded triangle, see Figure 12. The longitude will consist of u_j for each edge. The sum for each portion along the strand will be the longitude of the cusp. \square

Remark 4.4. For a link component in the projection plane that has half-twists, tracking the longitude is a bit trickier. A FAL with a half-twist and more than one component in the projection plane, the component in the projection plane which goes through an odd number of half-twists will still have meridian of length 1. The longitude will travel parallel to the projection plane except when it will pass a half-twist where it will then travel down/up to the other polyhedron thus it will increase its length by $\pm k\mu/2$ where k takes into account the direction of the half-twist and how many times it passes a half-twist. The cusp shape for the component will be the sum

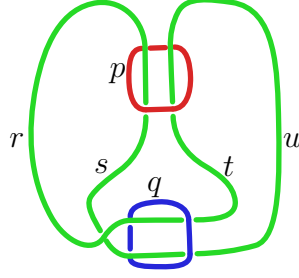


FIGURE 22. Borromean Ring FAL with half-twist.

of the edge labels plus half an integer, $\sum u_i \pm k \times \frac{1}{2}$, where the sign will depend on the direction of the half-twists. This is due to a shear, thus the cusp will not necessarily be rectangular. However, if the component goes through an even number of half-twists, then it will have a rectangular cusp, just the longitude won't be perpendicular to the real meridian—the cusp shape will be as if no half-twists are present. In addition, if a FAL has only one component in the projection plane then the cusp will be rectangular regardless if there is a half-twist present [14].

Experimentally, FAL with odd number of half-twists such that the presence of the half-twist reduces the number of components seem to be the ones impacted by the shear. Moreover, when there is one half-twist present the cusp shape will be $\sum u_i \pm 2$.

4.1. Examples.

4.1.1. *Borromean Ring FAL with a half-twist.* See Figure 22. Using the results from the Borromean Ring FAL without half-twist, we get

$$u_2 = u_3 = -\omega_1 = -\omega_2 = \pm \frac{i}{2}.$$

Thus there are three cusps: Cusp p with cusp shape

$$4\omega_2 = 4 \times \frac{i}{2} = 2i.$$

Cusp q with cusp shape

$$\frac{4\omega_1}{1 - 2\omega_1} = \frac{4 \times \frac{i}{2}}{1 - 2 \times \frac{i}{2}} = -1 + i.$$

The cusp shape for the single component in the projection plane, has rectangular cusp with longitude

$$u_1 + u_2 + u_3 + u_4 = 4 \times \frac{i}{2} = 2i.$$

4.1.2. *3 Pretzel FAL without half-twist.* Region \aleph : This is a three-sided region with shape parameters:

$$\xi_1 = \frac{-\frac{1}{4}}{u_1 u_3} = 1, \quad \xi_2 = \frac{-\frac{1}{4}}{u_1 u_2} = 1, \quad \xi_3 = \frac{-\frac{1}{4}}{u_2 u_3} = 1$$

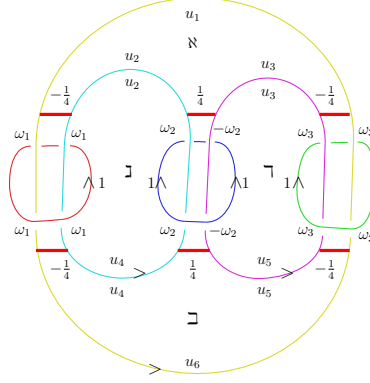


FIGURE 23. Three pretzel FAL.

solving gives us the relations

$$u_1 = u_2 = u_3 \quad \text{and} \quad u_1 = \pm \frac{i}{2}$$

Region 1: This is a three-sided region with shape parameters:

$$\xi_1 = \frac{-\frac{1}{4}}{u_4 u_6} = 1, \quad \xi_2 = \frac{-\frac{1}{4}}{u_4 u_5} = 1, \quad \xi_3 = \frac{-\frac{1}{4}}{u_5 u_6} = 1$$

solving gives us the relations

$$u_4 = u_5 = u_6 \quad \text{and} \quad u_4 = \pm \frac{i}{2}$$

Region 2:

$$\xi_1 = \frac{\omega_1}{u_4}, \quad \xi_2 = \frac{-\omega_2}{u_4}, \quad \xi_3 = \frac{-\omega_2}{u_2}, \quad \xi_4 = \frac{\omega_1}{u_2}$$

This is a four-sided region with equations:

$$\frac{\omega_1}{u_4} - \frac{\omega_2}{u_4} = 1, \quad \frac{-\omega_2}{u_4} - \frac{\omega_2}{u_2} = 1, \quad \frac{-\omega_2}{u_2} + \frac{\omega_1}{u_2} = 1, \quad \frac{\omega_1}{u_2} + \frac{\omega_1}{u_4} = 1$$

solving gives us the relations

$$u_2 = u_4, \quad \omega_1 = -\omega_2, \quad \text{and} \quad u_2 = 2\omega_1.$$

Region 3:

$$\xi_1 = \frac{-\omega_2}{u_5}, \quad \xi_2 = \frac{-\omega_3}{u_5}, \quad \xi_3 = \frac{-\omega_3}{u_3}, \quad \xi_4 = \frac{-\omega_2}{u_3}$$

solving gives us the relations

$$u_3 = u_5, \quad \omega_2 = \omega_3, \quad u_3 = -2\omega_2$$

all

$$u_i = \pm \frac{i}{2} \quad \text{and} \quad \omega_i = \pm \frac{i}{4}.$$

The cusp shapes for all 6 components are equal to i . The three crossing circles have cusp shape

$$4\omega_i = 4 \times \frac{i}{4} = i.$$

The component $s + y$ has cusp shape

$$u_1 + u_6 = 2 \times \frac{i}{2} = i.$$

The component $t + v$ has cusp shape

$$u_2 + u_4 = 2 \times \frac{i}{2} = i.$$

The component $u + x$ has cusp shape

$$u_3 + u_5 = 2 \times \frac{i}{2} = i.$$

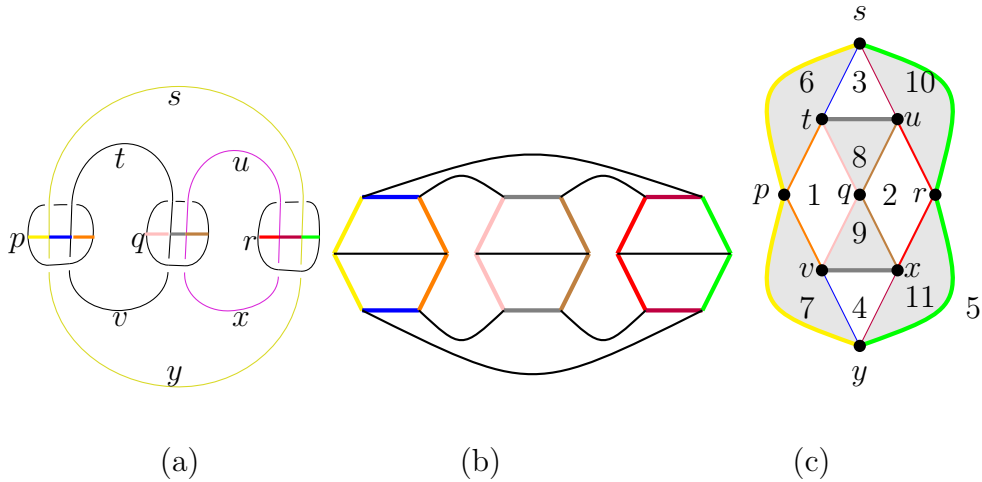


FIGURE 24. (a) $FALP_3$ with crossing geodesics colored. (b) T_{FALP_3} (c) P_{FALP_3}

4.1.3. *3 Pretzel FAL with half-twist.* In the diagram the five-sided region does not correspond to a five-sided ideal polygon, rather the polyhedral decomposition is the same as in the 3-pretzel without any half-twist, but the gluing of the faces change. Thus to find the cusp shapes we first obtain the parameters from the 3-pretzel without any half-twist and then calculate the cusps off those parameters and the above theorems. Using the information from the 3-pretzel FAL without a half-twist, we have $u_i = \pm \frac{i}{2}$ and $\omega_i = \pm \frac{i}{4}$. The cusp shape for the red crossing circle p is

$$\frac{4\omega_1}{1 - 2\omega_1} = \frac{4 \times \frac{i}{4}}{1 - 2 \times \frac{i}{4}} = \frac{-2}{5} + \frac{4i}{5}.$$

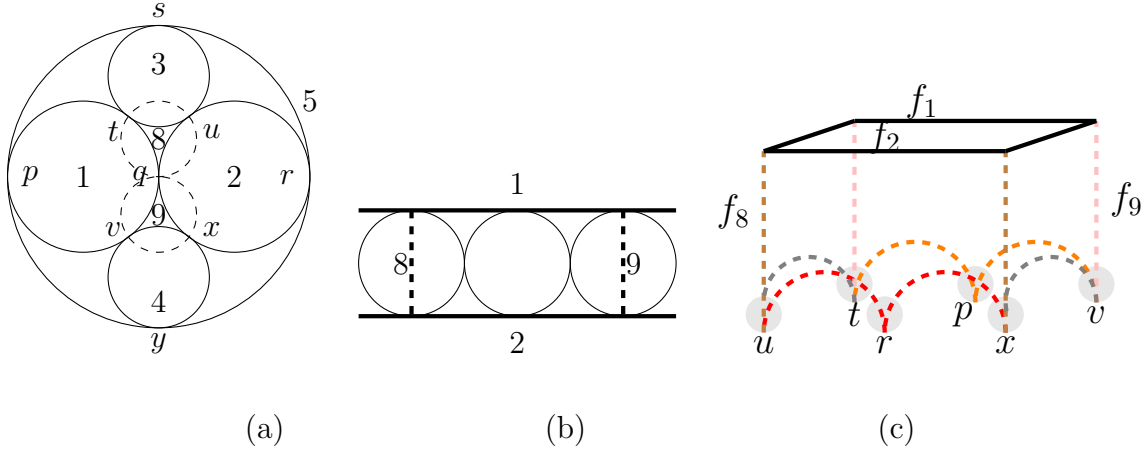


FIGURE 25. (a) White circle packing, with two dual shaded circles drawn on top. (b) View of rectangle in \mathbb{H}^3 formed by taking q to ∞ with view from ∞ (c) The faces of 1, 2, 8, and 9 in \mathbb{H}^3 , with view from vertical plane xz .

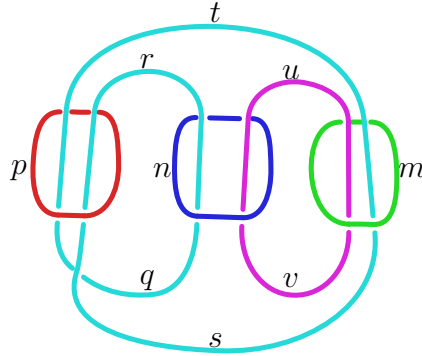


FIGURE 26. Diagram of 3-pretzel FAL with half-twist with components labeled.

The cusp shapes for the blue and green crossing circles n and m respectively are

$$4\omega_2 = 4 \times \frac{i}{4} = i.$$

The cusp shape for the light blue component in the projection plane $r + s + t + q$ is

$$u_2 + u_6 + u_1 + u_4 - 4\frac{1}{2} = 4 \times \frac{i}{2} - 2 = -2 + 2i.$$

The cusp shape for the pink component in the projection plane $u + v$ is

$$u_3 + u_5 = 2\frac{i}{2} = i.$$

5. APPLICATIONS

5.1. Invariant Trace Fields of FAL Complements. Let M be a complete orientable finite volume hyperbolic 3-manifold, then $M = \mathbb{H}^3/\Gamma$ where $\Gamma = \pi_1(M)$ (a Kleinian group) is a discrete subgroup of $PSL(2, \mathbb{C}) = Isom^+(\mathbb{H}^3)$. Let $\rho : SL(2, \mathbb{C}) \rightarrow PSL(2, \mathbb{C})$ be quotient map and let $\bar{\Gamma} = \rho^{-1}(\Gamma)$ [4].

Definition 5.1. The *trace field* $KM = K\Gamma$ is the field over \mathbb{Q} generated by all the traces of Γ , i.e. $K\Gamma := \mathbb{Q}(\{tr(\gamma) | \gamma \in \bar{\Gamma}\})$. The *invariant trace field* of Γ is $kM = k\Gamma := K\Gamma^{(2)}$ where $\Gamma^{(2)} := \langle \gamma^2 | \gamma \in \Gamma \rangle$.

It follows from Mostow-Prasad rigidity that KM and kM are number fields, i.e. finite extensions of \mathbb{Q} and are invariants of M .

Definition 5.2. M_1 and M_2 are *commensurable* if they have common finite-sheeted covers.

Theorem 5.3. [11] *The invariant trace field kM is an invariant of the commensurability class of M .*

Definition 5.4. Let M be a cusped hyperbolic 3-manifold. The field generated by the cusp shapes of all the cusps of M is called the *cuspidal field* of M , cM .

It follows from results of Neumann-Reid in [11] that cM is contained in kM and is a commensurability invariant. It is often the case that for a link complement M , $cM = kM$.

The polynomials we derive from the T-T method in terms of intercusp and translational parameters play a central role in studying the invariant trace fields of FAL complements.

If the images of the intercusp geodesics and translational geodesics are embedded in M , in which case we call them *intercusp arcs* and *cuspidal arcs* (respectively) then the following theorem holds.

Theorem 5.5. [12] *Suppose $X \subset M$ is a union of cuspidal arcs and pairwise disjoint intercusp arcs, where any intercusp arcs which are not disjoint have been bent slightly near intersection points to make them disjoint, and suppose $\pi_1(X) \rightarrow \pi_1(M)$ is surjective. Then the intercusp and translation parameters corresponding to these arcs generate kM .*

Theorem 5.6. *Let M be a FAL complement then $cM = kM$.*

Proof. kM is generated by all the meridian curves of the overstrands of the link diagram. Let X be the union of cuspidal arcs and pairwise disjoint intercusp arcs, see Figure 27. The meridians are all realized by the translation parameters, while the intercusp geodesics ensure that X is connected. For FALs the intercusp parameters ω_i and the translational parameters u_j are parameters of the intercusp arcs and cuspidal arcs, respectively, since FALs decompose into totally geodesic polyhedra. To show that $\pi_1(X) \rightarrow \pi_1(M)$ is surjective, we need to see that all the meridians are included. This is quite explicit, see Figure 27. The meridians for the crossing circles, the meridians for the components in the projection plane, and the meridian that runs around

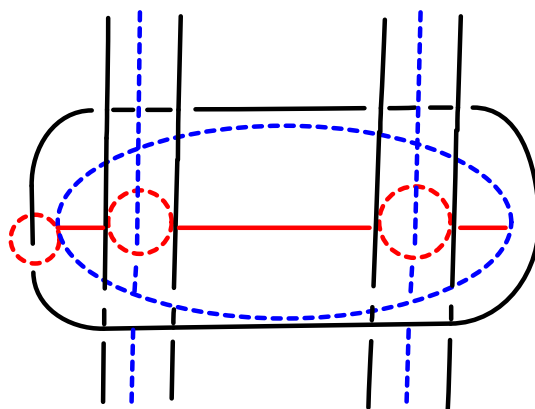


FIGURE 27. Meridians (red dashed curves), longitude curves (blue dashed curves), and intercusps geodesics (red solid lines)

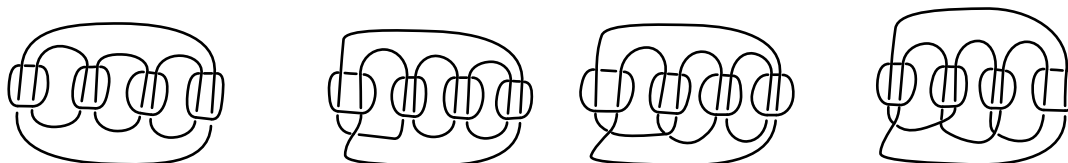


FIGURE 28. Non-isometric links $FALP_4$

the crossing circle in the projection plane are all combinations of the intercusps and translation parameters. By Theorem 5.5, ω_i s and the u_j s generate kM . Moreover by Theorems 4.1 and 4.3 ω_i s and u_j s generate the cusp field, thus $cM = kM$. \square

Theorem 5.7. *Let L_1 and L_2 be FAL that differ in half-twists and let $M_i = S^3 - L_i$, then $kM_1 = kM_2$.*

Proof. This follows from Theorem 4.1, the cusp shapes for FAL complements differing in half-twists have cusp shapes 4ω and $\frac{4\omega}{1\pm 2\omega}$ respectively, generating the same field. \square

FAL complements that differ in half-twists have the same volume and the same invariant trace fields, but are not isometric.

Corollary 5.8. *There exists an arbitrarily large set of links with complements having the same volume and same invariant trace fields yet are not isometric.*

Proof. The class of fully augmented pretzel links called $FALP_n$ have number of components ranging from $n + 1$ to $2n$ depending on half-twists, see Figure 29(a). $FALP_n$ without half-twists have $2n$ components, for each half-twist added the number of components decrease by 1. $FALP_n$ with $n - 1$ half-twists will have $n + 1$ components, see Figure 28. All of these links have the same volume as they decompose into the same ideal polyhedra, but are obtained by different gluings on the bowties. In addition, they have the same invariant trace field by Theorem 5.7. However, they are

non-isometric since they have different number of cusps which is an invariant of the link complement. \square

Remark 5.9. A very interesting question to study is the commensurability of these links. What happens to the commensurability of FAL when we add half-twists?

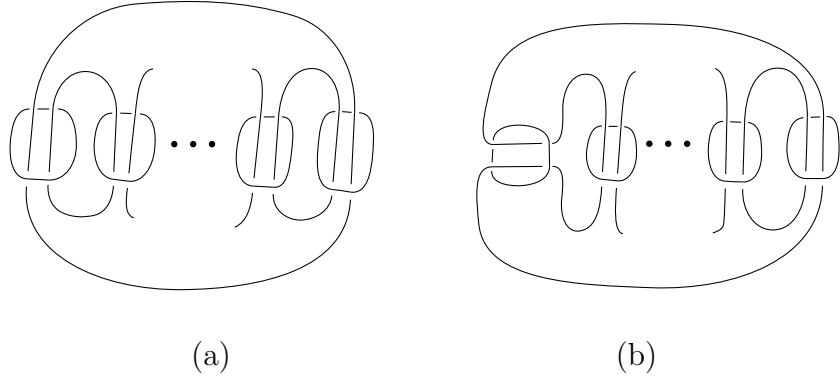


FIGURE 29. (a) $FALP_n$ (b) $FALR_n$

5.2. Commensurability of Pretzel FAL s. We denote the fully augmented link for the n -pretzel link $FALP_n$, see Figure 29(a). We explore the effects of a $\frac{\pi}{2}$ rotation on the left most crossing circle in a $FALP_n$ for $n \geq 3$. Let $FALR_n$ denote the link we obtain from $FALP_n$ by rotating the left most crossing circle by $\pi/2$, see Figure 29(b).

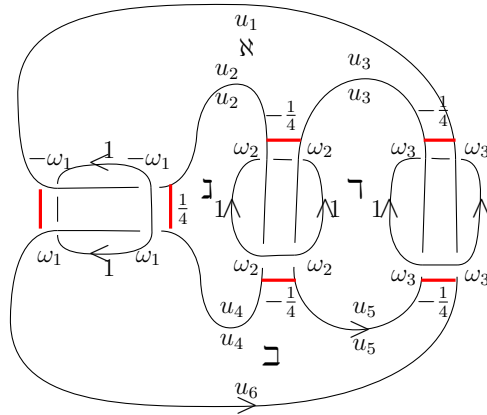


FIGURE 30. $FALR_3$

5.2.1. $FALP_3$ and $FALR_3$. We have studied $FALP_3$ in detail in §4. We now compute the T-T equations for $FALR_3$.

Region \aleph : We have shape parameters:

$$\xi_1 = \frac{-\omega_1}{u_1}, \quad \xi_2 = \frac{-\frac{1}{4}}{u_1 u_3}, \quad \xi_3 = \frac{-\frac{1}{4}}{u_3 u_2}, \quad \xi_4 = \frac{-\omega_1}{u_2}$$

This is a four-sided region with equations:

$$\frac{-\omega_1}{u_1} - \frac{\frac{1}{4}}{u_1 u_3} = 1, \quad \frac{-\frac{1}{4}}{u_1 u_3} - \frac{\frac{1}{4}}{u_3 u_2} = 1, \quad \frac{-\frac{1}{4}}{u_3 u_2} - \frac{\omega_1}{u_2} = 1, \quad \frac{-\omega_1}{u_2} - \frac{\omega_1}{u_1} = 1$$

solving gives us the relations

$$u_2 = u_1, \quad -2\omega_1 = u_2, \quad \text{and} \quad u_3 = -\frac{1}{2u_2}.$$

Region \beth : We have a three-sided region with shape parameters

$$\xi_1 = \frac{\omega_2}{u_2} = 1, \quad \xi_2 = \frac{\omega_2}{u_4} = 1, \quad \xi_3 = \frac{-\frac{1}{4}}{u_2 u_4} = 1 \quad \implies \quad u_2 = u_4 = \omega_2$$

$$\text{and } u_2^2 = -\frac{1}{4} \quad \implies \quad u_2 = \pm \frac{i}{2}.$$

$FALR_3$ has invariant trace field $x^2 + \frac{1}{4}$. It can be checked using snap [8] that both $FALP_3$ and $FALR_3$ are arithmetic. Since they have the same invariant trace field, they are commensurable. Note that they have the same volume yet they are not isometric links as they don't have the same number of components.

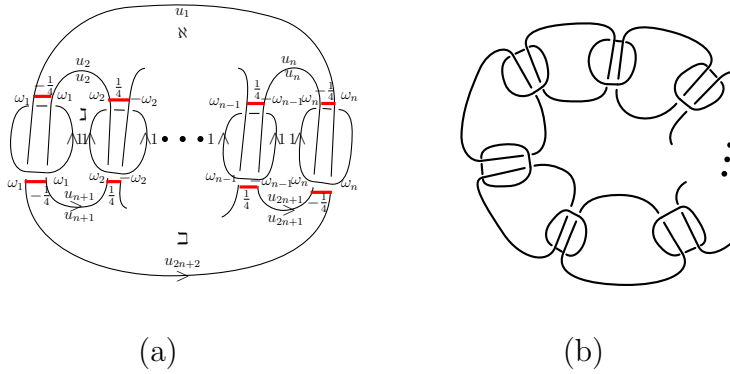


FIGURE 31. (a) $FALP_n$ with labels (b) Symmetric diagram of $FALP_n$

5.2.2. *T-T Polynomial for $FALP_n$ and $FALR_n$.* In this section we find a recurrence relation for the T-T polynomial for $FALP_n$ and $FALR_n$.

Theorem 5.10. *Let \aleph be the region in $FALP_n$ denoted in Figure 31(a). Let $C_n(x)$ be the $(2,1)$ entry of the matrix equation in Proposition 2.15, where $x = u_2$ is the edge parameter as shown in Figure 31(a). The T-T polynomial for $FALP_n$ is $C_n(x)$, which satisfies the recurrence relation*

$$C_n(x) = \frac{C_{n-2}(x)}{4} + xC_{n-1}(x)$$

for $n \geq 5$ where $C_3(x) = x^2 + 1/4$, $C_4(x) = \frac{x(2x^2+1)}{2}$.

Proof. From the symmetries in these links (see Figure 31(b)) and the shape parameter equations for the four-sided regions we have

- (1) $-\omega_1 = \omega_2 = \dots = \omega_n$
- (2) $u_2 = u_3 = \dots = u_n$

(3) and $-2\omega_i = u_j$ where $i, j \neq 1$ or $2n + 2$.

For simplicity let $u_2 = x$ and $u_1 = z$.

The smallest $FALP_n$ is when $n = 3$. Let $n = 3$ the matrix equation for Region \aleph is:

$$\begin{bmatrix} 0 & -\frac{1}{4} \\ 1 & 0 \end{bmatrix} \begin{bmatrix} 1 & x \\ 0 & 1 \end{bmatrix} \begin{bmatrix} 0 & \frac{1}{4} \\ 1 & 0 \end{bmatrix} \begin{bmatrix} 1 & x \\ 0 & 1 \end{bmatrix} \begin{bmatrix} 0 & -\frac{1}{4} \\ 1 & 0 \end{bmatrix} \begin{bmatrix} 1 & -z \\ 0 & 1 \end{bmatrix} = \begin{bmatrix} \frac{-x}{4} & \frac{1}{16} + \frac{xz}{4} \\ x^2 + \frac{1}{4} & -x^2z - \frac{x}{4} - \frac{z}{4} \end{bmatrix}$$

thus

$$C_3(x) = x^2 + \frac{1}{4}.$$

For $n = 4$ $FALP_4$ the matrix equation for Region \aleph is:

$$\begin{bmatrix} 0 & -\frac{1}{4} \\ 1 & 0 \end{bmatrix} \begin{bmatrix} 1 & x \\ 0 & 1 \end{bmatrix} \begin{bmatrix} 0 & \frac{1}{4} \\ 1 & 0 \end{bmatrix} \begin{bmatrix} 1 & x \\ 0 & 1 \end{bmatrix} \begin{bmatrix} 0 & \frac{1}{4} \\ 1 & 0 \end{bmatrix} \begin{bmatrix} 1 & x \\ 0 & 1 \end{bmatrix} \begin{bmatrix} 0 & -\frac{1}{4} \\ 1 & 0 \end{bmatrix} \begin{bmatrix} 1 & -z \\ 0 & 1 \end{bmatrix} = \\ \begin{bmatrix} -\left(\frac{x^2}{4} + \frac{1}{16}\right) & \frac{x^2z}{4} + \frac{x}{16} + \frac{z}{16} \\ \frac{x(2x^2+1)}{2} & -x^3z - \frac{x^2}{4} - \frac{xz}{2} - \frac{1}{16} \end{bmatrix}$$

thus

$$C_4(x) = \frac{x(2x^2+1)}{2}$$

For $FALP_{n-2}$ Region \aleph is a $(n-2)$ -sided region with matrix equation

$$\begin{bmatrix} 0 & -\frac{1}{4} \\ 1 & 0 \end{bmatrix} \begin{bmatrix} 1 & x \\ 0 & 1 \end{bmatrix} \left(\begin{bmatrix} 0 & \frac{1}{4} \\ 1 & 0 \end{bmatrix} \begin{bmatrix} 1 & x \\ 0 & 1 \end{bmatrix} \right)^{n-4} \begin{bmatrix} 0 & -\frac{1}{4} \\ 1 & 0 \end{bmatrix} \begin{bmatrix} 1 & -z \\ 0 & 1 \end{bmatrix} \\ = \begin{bmatrix} A_{n-2} & B_{n-2} \\ C_{n-2} & D_{n-2} \end{bmatrix} = \alpha \begin{bmatrix} 1 & 0 \\ 0 & 1 \end{bmatrix}$$

Now for $FALP_{n-1}$ Region \aleph is an $(n-1)$ -sided region with matrix equation

$$\begin{bmatrix} 0 & -\frac{1}{4} \\ 1 & 0 \end{bmatrix} \begin{bmatrix} 1 & x \\ 0 & 1 \end{bmatrix} \begin{bmatrix} 0 & \frac{1}{4} \\ 1 & 0 \end{bmatrix} \begin{bmatrix} 0 & 1 \\ -4 & 0 \end{bmatrix} \begin{bmatrix} A_{n-2} & B_{n-2} \\ C_{n-2} & D_{n-2} \end{bmatrix} = \begin{bmatrix} 0 & -\frac{1}{4} \\ -1 & x \end{bmatrix} \begin{bmatrix} A_{n-2} & B_{n-2} \\ C_{n-2} & D_{n-2} \end{bmatrix} \\ = \begin{bmatrix} A_{n-1} & B_{n-1} \\ C_{n-1} & D_{n-1} \end{bmatrix} = \begin{bmatrix} -\frac{C_{n-2}}{4} & -\frac{D_{n-2}}{4} \\ -A_{n-2} + xC_{n-2} & -B_{n-2} + xD_{n-2} \end{bmatrix}$$

Now for $FALP_n$ Region \aleph is an n -sided region with matrix equation

$$\begin{bmatrix} 0 & -\frac{1}{4} \\ -1 & x \end{bmatrix} \begin{bmatrix} A_{n-1} & B_{n-1} \\ C_{n-1} & D_{n-1} \end{bmatrix} = \begin{bmatrix} A_n & B_n \\ C_n & D_n \end{bmatrix} = \\ \begin{bmatrix} -\frac{C_{n-1}}{4} & -\frac{D_{n-1}}{4} \\ -A_{n-1} + xC_{n-1} & -B_{n-1} + xD_{n-1} \end{bmatrix}$$

Where $A_{n-1} = -\frac{C_{n-2}}{4}$, thus $C_n(x) = \frac{C_{n-2}}{4} + xC_{n-1}$. \square

In Table 2 below we compute $C_n(x)$ for some values of n . We list the factors of $C_n(x)$. The factor in bold corresponds to the invariant trace field, which is listed in the last column. We checked using pari-gp that every root of this factor lies in the invariant trace field.

Proposition 5.11. *It follows from the recurrence that the degree of $C_n(x) = n - 1$.*

Conjecture 5.12. *$C_n(x)$ satisfies the following conditions:*

- (1) *If n is prime then $C_n(x)$ is irreducible.*

C	T-T Polynomial	Invariant trace field
3	$(4x^2 + 1)/4$	$x^2 + 1$
4	$x(2x^2 + 1)/2$	$x^2 + 2$
5	$(16x^4 + 12x^2 + 1)/16$	$x^4 + 3x^2 + 1$
6	$x(4x^2 + 1)(4x^2 + 3)/16$	$x^2 - x + 1$
7	$(64x^6 + 80x^4 + 24x^2 + 1)/64$	$x^6 + 5x^4 + 6x^2 + 1$
8	$x(2x^2 + 1)(8x^4 + 8x^2 + 1)/16$	$x^4 + 4x^2 + 2$
9	$(4x^2 + 1)(64x^6 + 96x^4 + 36x^2 + 1)/256$	$x^6 + 6x^4 + 9x^2 + 1$
10	$x(16x^4 + 12x^2 + 1)(16x^4 + 20x^2 + 5)/256$	$x^4 - x^3 + x^2 - x + 1$
11	$(1024x^{10} + 2304x^8 + 1792x^6 + 560x^4 + 60x^2 + 1)/1024$	$x^{10} + 9x^8 + 28x^6 + 35x^4 + 15x^2 + 1$
12	$x(2x^2 + 1)(4x^2 + 1)(4x^2 + 3)(16x^4 + 16x^2 + 1)/512$	$x^4 + 4x^2 + 1$
13	$(4096x^{12} + 11264x^{10} + 11520x^8 + 5376x^6 + 1120x^4 + 84x^2 + 1)/4096$	$x^{12} + 11x^{10} + 45x^8 + 84x^6 + 70x^4 + 21x^2 + 1$
14	$x(64x^6 + 80x^4 + 24x^2 + 1)(64x^6 + 112x^4 + 56x^2 + 7)/4096$	$x^6 - x^5 + x^4 - x^3 + x^2 - x + 1$
15	$(4x^2 + 1)(16x^4 + 12x^2 + 1)(256x^8 + 576x^6 + 416x^4 + 96x^2 + 1)/16384$	$x^8 + 9x^6 + 26x^4 + 24x^2 + 1$
16	$x(2x^2 + 1)(8x^4 + 8x^2 + 1)(128x^8 + 256x^6 + 160x^4 + 32x^2 + 1)/2048$	$x^8 + 8x^6 + 20x^4 + 16x^2 + 2$
17	$(65536x^{16} + 245760x^{14} + 372736x^{12} + 292864x^{10} + 126720x^8 + 29568x^6 + 3360x^4 + 144x^2 + 1)/65536$	$x^{16} + 15x^{14} + 91x^{12} + 286x^{10} + 495x^8 + 462x^6 + 210x^4 + 36x^2 + 1$

TABLE 2. T-T polynomial and invariant trace field for $FALP_n$

(2) $C_m(x)|C_n(x)$ if and only if $m|n$.

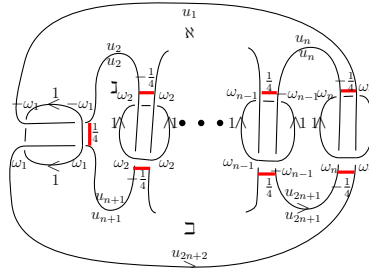


FIGURE 32. $FALR_n$ with labels

Computations for $FALR_n$:

For Region \mathfrak{J} we have a 3-sided region

$$\xi_1 = \frac{\omega_2}{u_2} = 1, \quad \xi_2 = \frac{\omega_2}{u_{n+1}} = 1, \quad \xi_3 = \frac{-\frac{1}{4}}{u_2 u_{n+1}} = 1,$$

\implies

$$u_2 = u_{n+1} = \omega_2 = \pm \frac{i}{2}.$$

From the similarities in the 4-sided regions we get the following equations

$$u_3 = \dots = u_n, \quad \omega_2 = \dots = \omega_n, \quad u_3 = 2\omega_2.$$

Without loss of generality let

$$\omega_2 = \frac{i}{2}, \quad \omega_1 = x, \quad u_1 = z.$$

Then Region \mathfrak{K} is a $(n + 1)$ -sided region with matrices equation

$$\begin{bmatrix} 0 & -\frac{1}{4} \\ 1 & 0 \end{bmatrix} \begin{bmatrix} 1 & i \\ 0 & 1 \end{bmatrix} \left(\begin{bmatrix} 0 & \frac{1}{4} \\ 1 & 0 \end{bmatrix} \begin{bmatrix} 1 & i \\ 0 & 1 \end{bmatrix} \right)^{n-3} \begin{bmatrix} 0 & -\frac{1}{4} \\ 1 & 0 \end{bmatrix} \begin{bmatrix} 1 & -\frac{i}{2} \\ 0 & 1 \end{bmatrix} \begin{bmatrix} 0 & -x \\ 1 & 0 \end{bmatrix} \begin{bmatrix} 1 & 1 \\ 0 & 1 \end{bmatrix} \begin{bmatrix} 0 & -x \\ 1 & 0 \end{bmatrix} \\ \begin{bmatrix} 1 & -z \\ 0 & 1 \end{bmatrix} = \alpha \begin{bmatrix} 1 & 0 \\ 0 & 1 \end{bmatrix}.$$

The $(2,1)$ -entry will give you a solution in $\mathbb{Q}(i)$ for all n . All the cusps other than the crossing circle that is rotated have equal cusp shapes of $2i$. To find the cusp shape for the cusp of the rotated crossing circle, solve the above equation and multiply the solution by 4.

Theorem 5.13. *Let $m, n \geq 3$, then $FALR_m$ and $FALR_n$ are commensurable.*

Proof. From Figure 34 we can see that $FALR_n$ is a $(n - 1)$ -sheeted cover of the Borromean rings. Hence $FALR_n$ is commensurable with the Borromean rings $FALR_3$. Since commensurability is an equivalence relation, $FALR_m$, which is a $(m - 1)$ -sheeted cover of the Borromean rings is commensurable with $FALR_n$. \square

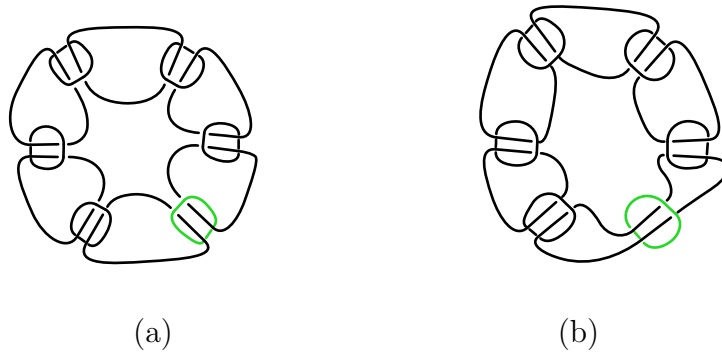


FIGURE 33. (a) Symmetric diagram of $FALP_6$ (b) $FALR_6$ with rotated crossing circle green

Corollary 5.14. *For $n \geq 3$, the invariant trace field for $FALR_n$ is $\mathbb{Q}(i)$.*

FIGURE 34. $FALR_6$ where green dot is vertical axis viewed from ∞ , Borromean Ring with green crossing circle viewed from ∞ .

Conjecture 5.15. (1) $FALP_n$ and $FALP_m$ are incommensurable for $n \neq m$.
 (2) For $n \geq 4$, $FALP_n$ and $FALR_n$ are incommensurable for all n .

Remark 5.16. For $n \neq m$, $FALP_n$ has different invariant trace field than $FALP_m$ by Conjecture 5.12. For the second part, by Conjecture 5.12 $FALP_n$ for $n > 3$ have invariant trace fields $\neq \mathbb{Q}(i)$, while the invariant trace field for all $FALR_n$ is $\mathbb{Q}(i)$, thus they are incommensurable.

5.3. Geometric Solutions to T-T Equations. The T-T method gives us a way to construct algebraic equations in variables, which then gives us a representation ρ_i in $PSL(2, \mathbb{C})$ with matrix entries in terms of root x_i of the T-T polynomial. Moreover, there exists a root x_0 of the T-T polynomial such that ρ_{x_0} is discrete and faithful, this solution will be the geometric solution.

For FALs all the non-real complex solutions lie in $k\Gamma$ thus to find the geometric solution we use Theorem 4.1, which states that 4ω will give us the cusp shape. We can therefore work backwards, use SnapPy to compute the cusp shape and see which solutions give us the cusp shape, thereby giving us the geometric solution.

Theorem 5.17. *Let L be a FAL, then the solution of the T-T polynomials which corresponds to the cusp shape is the geometric solution.*

Proof. The T-T polynomial for FALs can be written in a variable which is an edge parameter for a crossing circle, which is related to the cusp shape of that crossing circle. Due to Mostow-Prasad Rigidity the geometric structure of the manifold is unique. For fully augmented links, Theorems 4.1 and 4.3 show how the T-T polynomial gives us the cusp shape, which is a geometric invariant. Different solutions to the T-T polynomial would imply different choices of cusp shapes, which would contradict the uniqueness. Thus the solution to the discrete faithful representation must be the one that results in the correct cusp shape. \square

REFERENCES

- [1] Colin C. Adams. Thrice-punctured spheres in hyperbolic 3-manifolds. *Transactions of the American Mathematical Society*, 287(2):645, 1985.
- [2] Colin C Adams. Augmented alternating link complements are hyperbolic. *Lowdimensional topology and Kleinian groups (Coventry/Durham, 1984)*, 112:115–130, 1986.
- [3] Colin C. Adams. Waist size for cusps in hyperbolic 3-manifolds. *Topology*, 41(2):257 – 270, 2002.
- [4] Patrick J Callahan and Alan W Reid. Hyperbolic structures on knot complements. *Chaos, Solitons & Fractals*, 9(4):705–738, 1998.
- [5] E. Chesebro, J. DeBlois, and H. Wilton. Some virtually special hyperbolic 3-manifold groups. *ArXiv e-prints*, March 2009.
- [6] Marc Culler, Nathan M Dunfield, and Jeffrey R Weeks. SnapPy, a computer program for studying the geometry and topology of 3-manifolds, 2012.

- [7] David Futer, Efstratia Kalfagianni, and Jessica Purcell. Quasifuchsian state surfaces. *Transactions of the American Mathematical Society*, 366(8):4323–4343, 2014.
- [8] Oliver Goodman and W Neumann. Snap, a computer program for studying arithmetic invariants of hyperbolic 3-manifolds, 2001.
- [9] Marc Lackenby. The volume of hyperbolic alternating link complements. *Proc. London Math. Soc. (3)*, 88(1):204–224, 2004. With an appendix by Ian Agol and Dylan Thurston.
- [10] Walter D Neumann. Realizing arithmetic invariants of hyperbolic 3-manifolds. *Interactions between hyperbolic geometry, quantum topology and number theory*, 541:233–246, 2011.
- [11] Walter D Neumann and Alan W Reid. Arithmetic of hyperbolic manifolds. *Topology*, 90:273–310, 1992.
- [12] Walter D. Neumann and Anastasiia Tsvietkova. Intercusp geodesics and the invariant trace field of hyperbolic 3-manifolds. *Proc. Amer. Math. Soc.*, 144(2):887–896, 2016.
- [13] Jessica S. Purcell. *Cusp shapes of hyperbolic link complements and Dehn filling*. ProQuest LLC, Ann Arbor, MI, 2004. Thesis (Ph.D.)–Stanford University.
- [14] Jessica S Purcell. Meridians and generalized augmented links. *arXiv preprint math.GT/0703638*, 2007.
- [15] Jessica S. Purcell. An introduction to fully augmented links. In *Interactions between hyperbolic geometry, quantum topology and number theory*, volume 541 of *Contemp. Math.*, pages 205–220. Amer. Math. Soc., Providence, RI, 2011.
- [16] Morwen Thistlethwaite and Anastasiia Tsvietkova. An alternative approach to hyperbolic structures on link complements. *Algebr. Geom. Topol.*, 14(3):1307–1337, 2014.
- [17] William P Thurston. *The geometry and topology of three-manifolds*. Notes from Princeton University, 1979.
- [18] Jeff Weeks. Computation of hyperbolic structures in knot theory. In *Handbook of knot theory*, pages 461–480. Elsevier, 2005.

DEPARTMENT OF MATHEMATICS, SCIENCE, AND TECHNOLOGY, TEACHERS
COLLEGE, COLUMBIA UNIVERSITY, NEW YORK, NY

E-mail address: crf51@tc.columbia.edu